University of Stavanger

Faculty of Science and Technology

MASTER'S THESIS

Study program/ Specialization: **Master of Sciences in Petroleum Engineering** **Production Engineering**	Spring Semester, 2014 **Open**
Writer: **Hilda CHOQUE FLORES**	…… (Writer's signature)

Faculty supervisor: Jann Rune Ursin

External supervisor(s):

Thesis title:

CO_2 SEQUESTRATION IN GAS-CONDENSATE RESERVOIRS

Credits (ECTS): 30

Key words: **Gas-condensate reservoirs** **CO_2 Injection** **Displacement Models** **CO_2 Sequestration**	Pages: ……78…… + Enclosure: …….. Stavanger, **July 30th, 2014** Date/year

CO_2 SEQUESTRATION IN GAS-CONDENSATE RESERVOIRS

ABSTRACT

In this thesis, it is being analyzed effects of carbon dioxide (CO_2) injected into a retrograde gas reservoir to enhance liquid production from such reservoirs while simultaneously sequestering amounts of CO_2. Mixing between carbon dioxide (injection fluid) and gas condensate (resident gas) is limited due to high density and viscosity of carbon dioxide relative to gas condensate.

Simulations for Carbon Dioxide injection were done in idealized reservoir using 3 different Displacement Models and different correlations to model CO_2 properties. This analysis includes a study of carbon dioxide physical properties into the system of CO_2-Gas Condensate. In order to diminish discrepancies for modeling of carbon dioxide physical properties mainly for its supercritical state, it has been plotted data and compared with actual data for Carbon Dioxide Properties which shows very good approximations for the different correlations chosen when developing the in-house simulator.

Additionally, carbon dioxide injection may offer other benefits such as pressure support, important feature for gas condensate reservoirs.

DEDICATION

I dedicate my Master Thesis to my parents Alejandro and Hilda. My mother´s dream comes true when finishing this Master Thesis; in the future I wish to see her in Paradise. I really thank to my father Alejandro who is with me in each step of my life for his affection, which gave me forces to make this work, his effort through all those years that were rewarded and his trust deposited in me was very special and important.

A special dedication to my loving siblings: Esther, Luz Marina, Vladimir, Jocelyn and Zoraida for their motivation demonstrated along those years and to my nephew Brian and niece Kaye who made my life be full of happiness with all of their mischievousness.

All of you have my unconditional affection,

Hilda CHOQUE FLORES

ACKNOWLEDGEMENT

First of all, I am really grateful to Almighty God. His love is infinite and He is infinitely merciful, good, faithful, just. May His light always guide my way and give me wisdom to discern the ways in life.

I would like to express my most sincere gratitude to my advisor Professor Jann Rune Ursin for his patience, time, expertise and guidance through all time of writing this Master Thesis and giving me the opportunity to work in this exciting project.

Moreover, I would like to thank to Eng. Terje Froiland at the University of Stavanger and Eng. Hermas Herrera at the Universidad Mayor de San Andrés for their motivation, encouragement and continuous cooperation during my studies in Norway. It is highly appreciated.

A special feeling of gratitude to the members of the EnPe Project for giving me this great opportunity to study my Master Degree in Stavanger, Norway allowing me to conduct this research and providing me with further knowledge.

Furthermore, I thank to my fellow in Norway: Diana Pavón, Héctor Silva, Rawt Abdwlla, Insea Seeram, Antonio Heredia, Amaru Gutiérrez for their enthusiasm, generosity and support while studying together in those sleepless nights, for all fun we had in those two years. Every one of you made this time at the University of Stavanger in a time of feeling affection. I really wish an endless friendship with all of you.

Special thanks to my friends in Bolivia: Karla Jiménez, Mérida Cahuaya and Dana Vallejos for their unforgettable friendship even in the distance it was like having them besides me and a piece of my country in my heart.

I wish to thank the committee members for their countless hours of reading and precious time.

Finally, I would also to express my appreciation to every one of my professors, administrators at the Department of Petroleum Engineering and Faculty of Sciences and Technology for their assistance, help and feedback in the completion of this research and this enjoyable experience in this beautiful land.

TABLE OF CONTENTS

LIST OF FIGURES

LIST OF TABLES

CO_2 SEQUESTRATION IN GAS-CONDENSATE RESERVOIRS

CHAPTER 1

INTRODUCTION

It has been suggested the idea of injecting carbon dioxide into depleted gas reservoirs. They have demonstrated over geological time to have great features to storage large quantities of gas, to prevent its escape and to be good available candidates to hold large volumes for carbon sequestration.

Among its promising characteristics, injection of carbon dioxide enhances gas recovery by means of *displacement* analogous to a water flooding and *repressurization* of retrograde gas reservoirs which is fundamental to limit entrance into retrograde region.

Carbon Dioxide is a promising injection fluid in gas condensate reservoirs due to large density and viscosity difference between gas condensate (resident gas) and CO_2 (injection fluid) that effectively will help to enhance gas recovery avoiding mixing, a main concern for degradation of value of remaining resident gas. Moreover, it is relatively high viscosity relative to resident gas makes a favorable mobility ratio for displacement and a less tendency to fingering, a main concern for displacement of injection fluid.

It was extended the old version of the in-house simulator to include CO_2 injection while monitoring displacement process from the injection well. The reservoir properties and actual conditions are given in Table 10 and Table 11.

Furthermore, it was simulated different scenarios for injection of carbon dioxide at different stages of the gas condensate reservoir lifetime.

OBJECTIVE

The purpose of this Thesis is to show analysis of carbon dioxide displacement into a gas condensate reservoir to provide a foundation for further study of possible future implementation of CO_2 as a promise injection fluid.

This analysis includes a study of carbon dioxide physical properties into the system of CO_2-Gas Condensate.

CO2 SEQUESTRATION IN GAS-CONDENSATE RESERVOIRS

CHAPTER 2

THEORETICAL BACKGROUND

2.1. Darcy´s Law: Permeability

Henry Darcy investigated flow of water in 1856 through sand filters used for water purification. Through his observations, it was noticed that fluid of flow was directly proportional to a pressure gradient which then resulted in:

$$q = KA\frac{\left(h_2 - h_1\right)}{L} \qquad \text{Equation 1}$$

In which q was the volumetric flow rate of water flowing downward in the cylindrical sand pack with a length L through a cross sectional area A; h_1 and h_2 are hydraulic head respect to the datum of water for the manometer located at the inlet and outlet ports. It was found a constant of proportionality "K" a characteristic of the medium called "hydraulic conductivity". Moreover, movement of fluid was due to the difference in potential energy; one of them being *fluid pressure* and *elevation* in which plays role gravity force. With a relationship between hydraulic head and pressure is possible to calculate pressure in the flow path at any point and is written as:

$$\Phi = \frac{P}{\rho} + gz = gh \qquad \text{Equation 2}$$

ϕ: total potential per unit mass
g: gravity acceleration
P: pressure
ρ: density of fluid in question
z: elevation of a point in the system

In differential form and substituting Equation 2 into Equation 1:

$$q = \frac{K}{g}A\frac{d}{dl}\left(\frac{P}{\rho} + gz\right) \qquad \text{Equation 3}$$

Then posterior experiments with a constant fluid potential gradient concluded that other fluid properties can also cause effects on flow rate such as grain diameter d and fluid viscosity μ; c is a constant of proportionality.

$$K = \frac{cd^2\rho g}{\mu}$$

Into Equation 3:

$$q = -\frac{k}{\mu} A\left(\frac{dP}{dl} + \rho g \frac{dz}{dl}\right) \qquad \text{Equation 4}$$

k: permeability of porous medium. Equation 4 is the well-known Darcy´s Law applied for:

A. Steady State
B. Laminar flow
C. Incompressible fluid
D. Homogenous and isotropic porous medium

The negative sign introduced into Equation 4 results from measuring distance and pressure in the same direction; then, gradient in parentheses is negative for the flow to move in the same direction from high to lower potential; for horizontal flow when z=0, (P_2-P_1) gives a negative value since pressure P_1 is higher than pressure P_2.

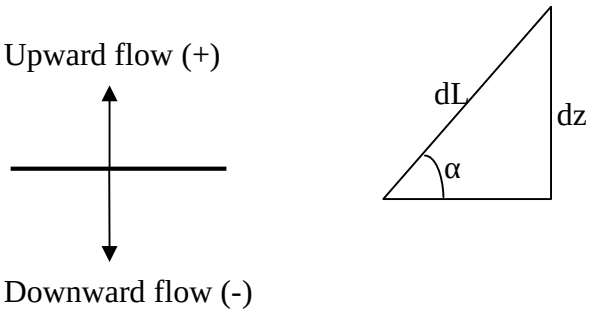

It can be substituted $\sin\alpha = \frac{dz}{dl}$ for elevation gradient for any flow angle α.
Sign convention is such that upward flow is positive (sin 90=1) and downward flow is negative (sin -90= -1). Introduced for Darcy´s Law at any angle of flow α:

$$q = -\frac{k}{\mu} A\left(\frac{dP}{dl} + \rho g \sin\alpha\right) \qquad \text{Equation 5}$$

2.2. Darcy's Law in Differential Form

In Section 2.1., it was discussed Darcy´s Law over a finite length, now it is given differential form of Darcy´s Law which is used to find different flow relations of different fluid types and for several geometries.

As it was seen Equation 4 was found with experiments based in potential drop, similar to pressure drop that was measured over a finite length L in that sandpack with permeability k. For an incompressible fluid in linear flow with viscosity μ flowing through the sandpack, the flow rate is given by:

$$q = \frac{kA\Delta P}{\mu L}$$ Equation 6

In which superficial velocity $u = \frac{q}{A}$.

The limit of pressure difference given over a length of flow Δx, it is the derivative with respect to length:

$$\lim_{\Delta x \to 0} \frac{p(x+\Delta x) - p(x)}{\Delta x} = \frac{dP}{dx}$$ Equation 7

This gives the Darcy´s Law in differential form in Equation 8. This can be integrated to compute Darcy´s Law for several flow geometries and various fluid types. The negative sign is introduced because flow direction is opposite to direction of pressure change. Similar as Equation 4.

$$u_{sup} = u = -\frac{k}{\mu}\frac{dP}{dx}$$ Equation 8

2.3. Integrated Forms of Darcy's Law: Incompressible Fluids

In the given equations lines above, pressure gradient is proportional to volume flow rate. In steady state flow, mass flow rate is constant. For incompressible fluids, volume flow rate is constant but for compressible fluids, this varies, the integrated form of Darcy´s Law will be given considering linear flow in this Thesis:

$$q = -\frac{kA}{\mu B}\frac{dP}{dx}$$ Equation 9

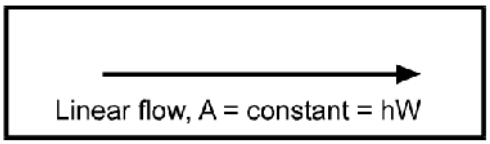

It was introduced *B* formation volume factor which converts from volume at standard conditions, surface or reference condition: stock tank barrel, to reservoir conditions, subsurface condition: reservoir barrel.

2.3.1. Linear Flow

For linear flow over a finite length L, Equation 9 can be integrated:

$$q\int dx = -\frac{kA}{\mu B}\int dP$$

$$q\int_0^L dx = -\frac{kA}{\mu B}\int_{P(0)}^{P(L)} dP$$

$$q \times (L-0) = -\frac{kA}{\mu B}\left[P(L) - P(0)\right]$$

$$q = -\frac{kA[P(L) - P(0)]}{\mu BL} \qquad \text{Equation 10}$$

When flow goes from 0 to L, it means pressure is greater at 0 than at L, the result of the difference in brackets is negative and the opposite when flow goes from L to 0; sign convention is right. Equation 10 is similar to Equation 6, Darcy´s Law equation, only that B formation volume factor is introduced and the sign in pressure drop and flow direction is now considered more carefully. This integrated flow equation can be used for prediction of steady-state flow of incompressible fluids.

Linear flow can be a good approximation for far flow of wells in reservoirs or between wells when studying a pattern flood, mostly in core floods. In this Thesis, it is considered linear flow. The function of distance *x* for pressure in linear flow dictates the flow geometry.

2.4. Integrated Forms of Darcy's Law: Gases

For gases, the B formation volume factor is:

$$B = \frac{P_{sc} Tz}{PT_{sc} z_{sc}} \qquad \text{Equation 11}$$

Equation 11 into differential form of Darcy´s Law Equation 9 for B:

$$q = -\frac{kA}{\mu B}\frac{dP}{dx}$$

$$= -\frac{kA}{\mu \frac{P_{sc} Tz}{PT_{sc}}}\frac{dP}{dx}$$

$$q = -\frac{kT_{sc} AP}{\mu TzP_{sc}}\frac{dP}{dx}$$

This last equation can be integrated:

$$\int_0^L q\,dx = -\int_{P_0}^{P_L} \frac{kT_{sc} A}{\mu TzP_{sc}} P\,dP$$

μ Viscosity and z compressibility factor changes with pressure i.e., are functions of pressure. According to Craft et al. those can be assumed almost constant:

$$q\int_0^L dx = -\frac{kT_{sc}A}{\mu TzP_{sc}}\int_{P_0}^{P_L} P\,dP$$

Integrating it:

$$q = -\frac{kT_{sc}A\left(P_L^2 - P_0^2\right)}{2\mu TzP_{sc}L} \qquad \text{Equation 12}$$

As it was mentioned Craft et al., analyzed behavior at relatively low and relatively high pressure to approximate the previous integrals and give good approximations for flow equations. Behavior of viscosity and compressibility factor at low pressure shows both are approximately constant as well as high pressure. Behavior at intermediate values of pressure is more complicated.

At low pressure for flow of gases, gas flow rate is directly proportional to the squared difference of pressure different than the difference of pressure as in flow of liquids. At high pressure, gas flow is similar to liquid flow, since gas compressibility is small.

It also good known, the preferred method for flow of gases with the transformation named real gas pseudo pressure, with some other calculations it is simpler and it is not necessary to use those approximations for low pressure (below 1000 psi) and high pressure (above 6000 psi). For ideal gases, compressibility factor z is 1 one and viscosity μ is not a function of pressure, then Equation 12 can be used when analyzing gases which behaves near ideal gases, PVT behavior.

The following assumptions are given viscosity μ, compressibility factor z, permeability k and Temperature T is constant. Moreover, viscosity and compressibility are evaluated at the mean pressure.

2.5. Carbon Dioxide Injection Process into Gas Condensate Reservoirs

The behavior of gas condensate reservoirs as pressure decreases, lighter components are being produced whilst the heavier components of the gas condense, rule the composition of retrograde liquid fluid during depletion. Therefore, depleted retrograde gas reservoirs may contain "condensates", a portion of which can be recovered by means of CO_2 injection. In those reservoirs where a large vertical relative to lateral extent, density effects (gravity forces) could be exploited by injecting CO_2 deep in the reservoir.

The CO_2 is captured, then compressed to a nearly liquid state and transported via pipeline to a gas condensate field for permanent sequestration while Enhancing Condensate Recovery (ECR).

The CO_2 is injected into its supercritical state deeper underground, travels down the wellbore (injection well) to a location where a rock formation provides a safe carbon dioxide sequestration whilst exploiting benefits of CO_2 injection.

This injection of supercritical CO_2 deep into reservoir through an injection well will cause its re pressurization and displacement of gas condensate for future production through a production well separated some distance further.

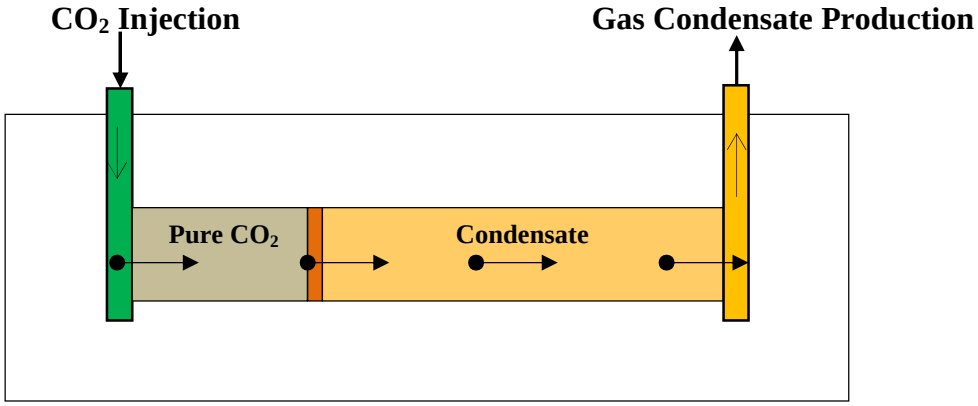

Figure 1 Two-dimensional Scheme of simulation domain for the Injection of Carbon Dioxide

CO_2 injection acting to re pressurize the reservoir to a level above to turn the remaining retrograde liquid mobile. Among the mixing process, pressure diffusivity is typically three –five orders of magnitude larger than molecular diffusivity making re pressurization occur much faster than mixing by molecular diffusion, a main feature in this thesis to assume non mixing between gas condensate (resident gas) and carbon dioxide (injection fluid) at reservoir conditions.

At operational level, for an Immiscible Injection Process, the mixing process of both "existing condensate gas" and "injected CO_2" can be controlled by operational strategies and taking advantage of the density difference of CO_2 relative to condensate gas in the reservoir.

The much denser and more viscous pure CO_2 relative to gas condensate causes to underride in the reservoir. Furthermore, this makes a favorable mobility ratio displacement diminishing usually tendency to interfinger. "Being fingering a hydrodynamic instability that occurs when a higher mobility fluid displaces a low mobility fluid" (Guillermo Calderon Leonid Surguchev).

Later time, the CO_2 will flow preferentially through "high permeability paths" causing reduction of condensate recovery as liquid retrograde is not efficiently swept in the low permeability regions. Therefore, earlier breakthrough of injected CO_2 which occurs in the high permeability zones will limit economically amounts of recoverable condensate.

Moreover, during production while pressure reduction takes place, the CO_2 from supercritical state can change to vapor phase with significant expansion.

In the aim of reservoir repressurization when CO_2 is detected in the producer well this indicates shut-in it and continue injecting supercritical CO_2 until to reach the original reservoir pressure. This indicates the end of injection and the reservoir would contain mostly carbon dioxide occupying pore spaces i.e., carbon dioxide has been sequestered.

2.6. Carbon Dioxide Sequestration into Gas Condensate Reservoirs

CO_2 is being injected into its supercritical state which minimizes any possibility of its escape from reservoir. The subsurface and surface pressure, bottom-hole and wellhead injection pressure respectively, must be such that carbon dioxide is maintained in this state and prevented to phase change in any part of its journey down wellbore.

As carbon dioxide injection process takes place, CO_2 becomes trapped into the pore spaces of a rock formation with a cap rock acting as a physical barrier in the same way as millions of years ago to trap gas which permits entrapment of CO_2 and prevents its escape.

There are three trapping mechanisms which ensure CO_2 remains safely stored in the reservoir: *Physical trapping, Dissolution and Mineralization*.

In the first, carbon dioxide which is stored in the porous geological formation will try to move upwards but it is stopped by the solid cap rock above it. In the second, carbon dioxide will dissolve into brine water found in the storage location. In the third, CO_2 will react with other minerals to form solid rocks like limestone. This means reaction with natural minerals contained into the rock formation to form stable minerals such as calcium carbonate. In this way, carbon dioxide cannot reenter into the carbon cycle that makes carbon dioxide sequestration be safe.

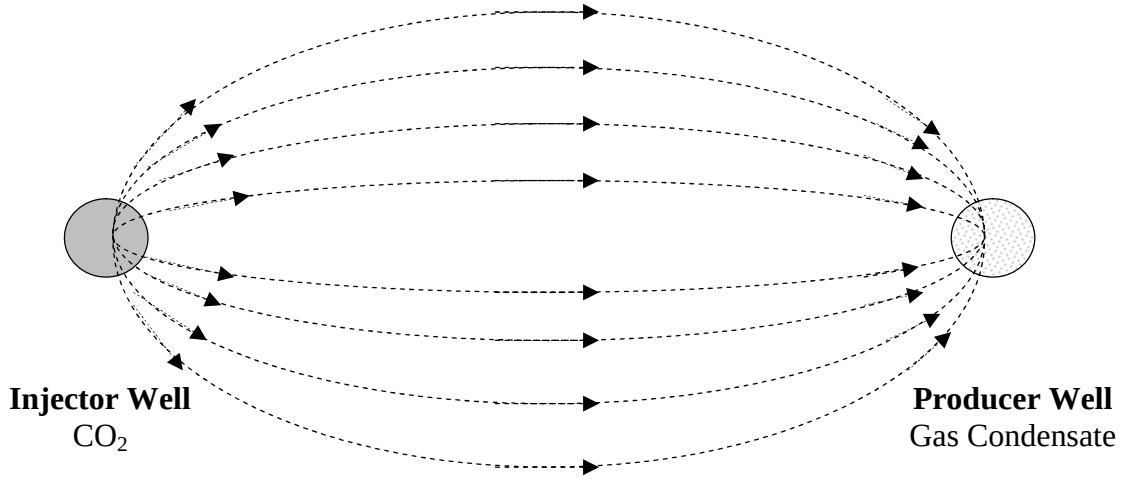

Figure 2 Displacement of Carbon Dioxide from Injector Well to Producer Well

2.7. Permeability role in Carbon Dioxide Injection

Absolute permeability assigned for simulation, see Appendix 4, characterizes it into "a good permeable rock" Table 1. In general, permeability heterogeneity; *vertical permeability and horizontal permeability*, will tend to create fast flow paths accelerating breakthrough Figure 3.

If equal effective permeability to CO_2 and gas condensate is assigned, it will lead to model injected CO_2 moves as faster as resident gas which in reality due to great differences in physical properties between them not to exploit this important feature of carbon dioxide as injection fluid. Then, if it is characterized with a high permeability value, CO_2 finds fast flow through

permeability bodies, this accelerates CO_2 breakthrough. Next, repressurization benefit will seem much slower process than expected. In essence, CO_2 injection helps to repressurized whole reservoir.

Classification	Permeability [mD]
Poor	< 1
Low	1-20
Medium	20-50
Good	50-200
Excellent	> 200

Table 1 Permeability Values and Classification

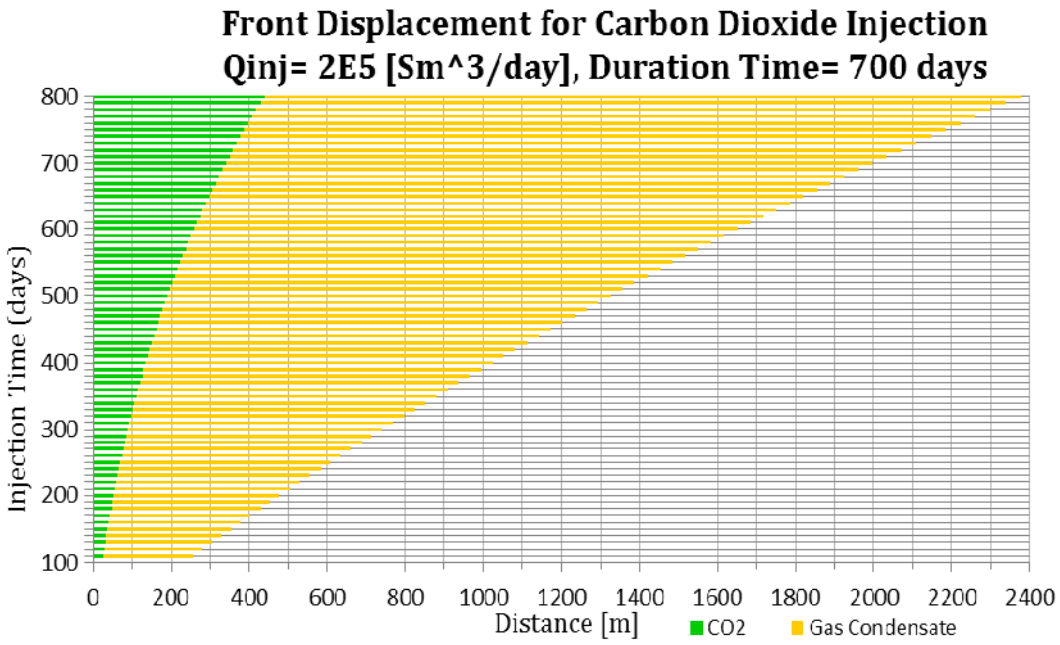

Figure 3 Breakthrough at Day 660 for Carbon Dioxide Injection Qinj= 200 000 [Sm^3/day]
Distance between Producer Well PCOGAS 1 and Injector Well ICOGAS 1= 300 [m]

2.8. Physical Properties

As can be seen in the Phase Diagram for CO_2 in Figure 4, for the present study, supercritical conditions for carbon dioxide prevails at reservoir conditions, once, pressure declines further, it can be changed to gas phase.

Comparing properties among gas condensate and carbon dioxide, CO_2 is much denser and more viscous than resident gas. CO_2 will have higher injectivity compared with water as a fluid injection due to its lower value of viscosity; however, tend to underride existing resident gas as water due to its high value of density.

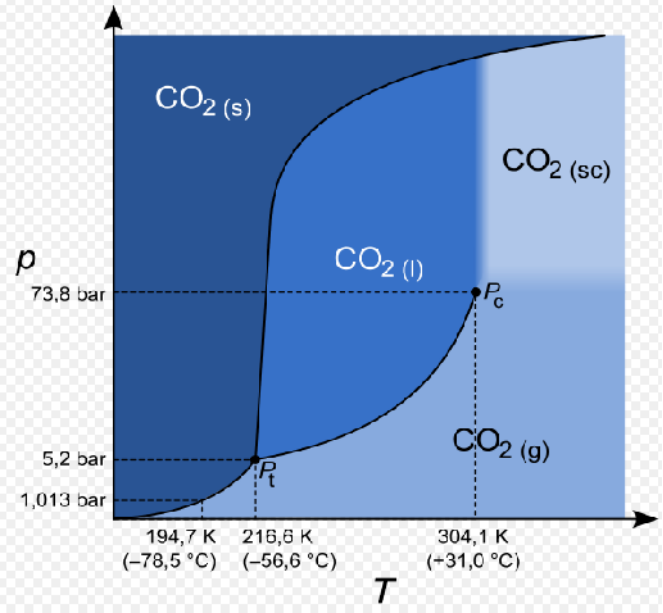

Figure 4 Carbon Dioxide Pressure-Temperature Phase Diagram
P: Pressure; T: Temperature; s= solid; l= liquid; sc= supercritical; g=gas;
Source: Wikimedia

In Figure 5 and 6 are the density and viscosity of gas condensate and carbon dioxide calculated in the in-house simulator ECLIPSE IDE UiS at actual reservoir conditions of pressure and temperature.

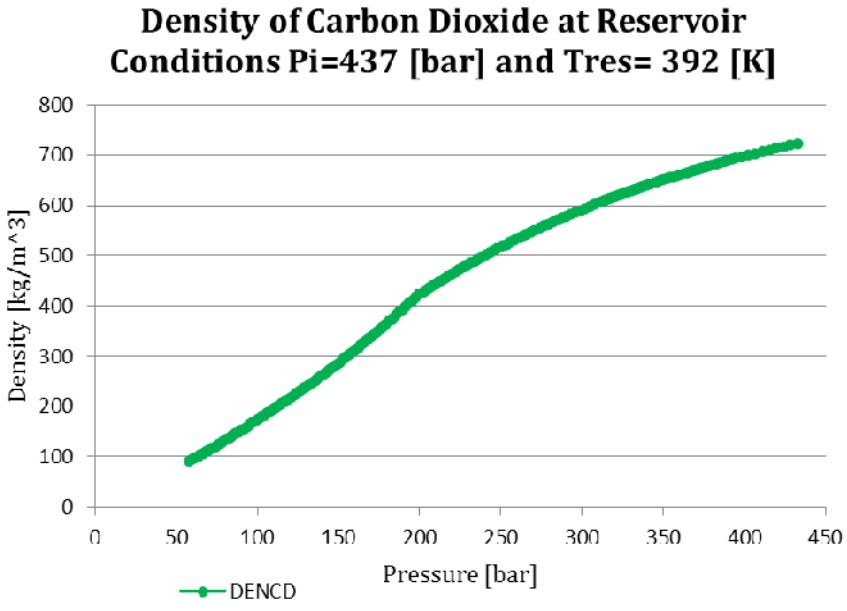

Figure 5 Density of Carbon Dioxide predicted by ECLIPSE-IDE at Reservoir Conditions
using Liang Biao Correlation

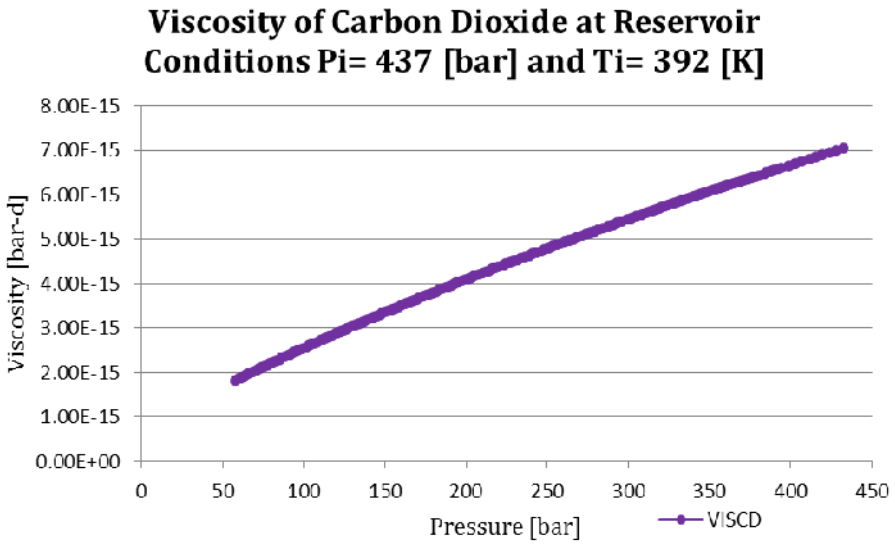

Figure 6 Viscosity of Carbon Dioxide predicted by ECLIPSE-IDE at Reservoir Conditions *using Heydaryan et al. Correlation*

2.8.1. Modelling of Carbon Dioxide Properties

2.8.1.1. Density of Carbon Dioxide

It was necessary to find a proper correlation to model carbon dioxide density, this is a very important property which helps to describe displacement process for CO_2 Injection. There was special attention to model properly supercritical region for carbon dioxide where it is not a distinction between phases, as density for carbon dioxide shows great changes among different states.

It has been needed some correlation that is function of pressure and temperature to model carbon dioxide density. Nowadays due to wide applications of supercritical fluids in different industrial fields, estimation of their fluid properties is very important. In literature among few available correlations for density and different correlations for viscosity, it has been chosen the two most recent and updated correlations for the prediction of supercritical carbon dioxide such as Bahadori et al. [1] and Liang Biao [2].

A. Bahadori et al. Correlation

It is a new correlation for predicting density of carbon dioxide. It accurately works for pressures between 25 [bar] and 700 [bar] and temperature range of 293 – 433 [K].

Their proposed methodology was to identify a polynomial equation able to correlate density carbon dioxide which includes reduced temperature and reduced pressure (inlet properties); the resultant outcome varies with temperature and pressure. A quantitatively estimation of the trend of outcomes was made assuming that “the best-fit polynomial equation of a given type is the one that has the minimal sum of the deviations squared (least square error) from a given set of data including temperature and pressure” [3].

Equation 13 presents the new developed correlation for predicting CO_2 density as a function of pressure and temperature, the units of density is kg per cubic meter, temperature T is in Kelvin and pressure P is in bar:

$$\rho = \alpha + \beta T + \gamma T^2 + \theta T^3 \qquad \text{Equation 13}$$

Where:

$$\alpha = A_1 + B_1 P + C_1 P^2 + D_1 P^3 \qquad \text{Equation 14}$$

$$\beta = A_2 + B_2 P + C_2 P^2 + D_2 P^3 \qquad \text{Equation 15}$$

$$\gamma = A_3 + B_3 P + C_3 P^2 + D_3 P^3 \qquad \text{Equation 16}$$

$$\theta = A_4 + B_4 P + C_4 P^2 + D_4 P^3 \qquad \text{Equation 17}$$

The tuned coefficients for Equation 14 to 17 are given in Table 2 and 3.

Coefficient	A	B	C	D
1	208980.0973	-14562.8633	288.5813588	-1.59710385
2	-1675.18235	116.7995543	-2.31558333	0.01284012
3	4.450600951	-0.31043015	0.006157719	-3.4203E-05
4	-0.00391984	0.000273497	-5.428E-06	3.01957E-08

Table 2 Tuned coefficients for Bahadori et al. Correlation 25 bar < P < 100 bar [1]

Coefficient	A	B	C	D
1	105329.3651	-939.644851	2.397414334	-0.00181905
2	-825.33835	7.618125849	-0.01963564	1.49766E-05
3	2.135712083	-0.02023129	5.27213E-05	-4.0436E-08
4	-0.00182796	1.7683E-05	-4.6534E-08	3.58671E-11

Table 3 Tuned coefficients for Bahadori et al. Correlation 100 bar < P < 700 bar [1]

Bahadori et al. compared reported data [3] with their results; the new developed correlation has a good agreement between the prediction results and observed values.

Besides the results that the author shows in his own work, to check validity of Bahadori et al. correlation for the present work, it was evaluated for different conditions every 10 [°F] according to available Reported Data [4] from 60 [°F] or T= 288 [K] and 180 [°F] or T= 355 [K], it was chosen 2 different conditions one, nearly entrance of supercritical region at T=305 [K] and two, a high temperature at T=355 [K].

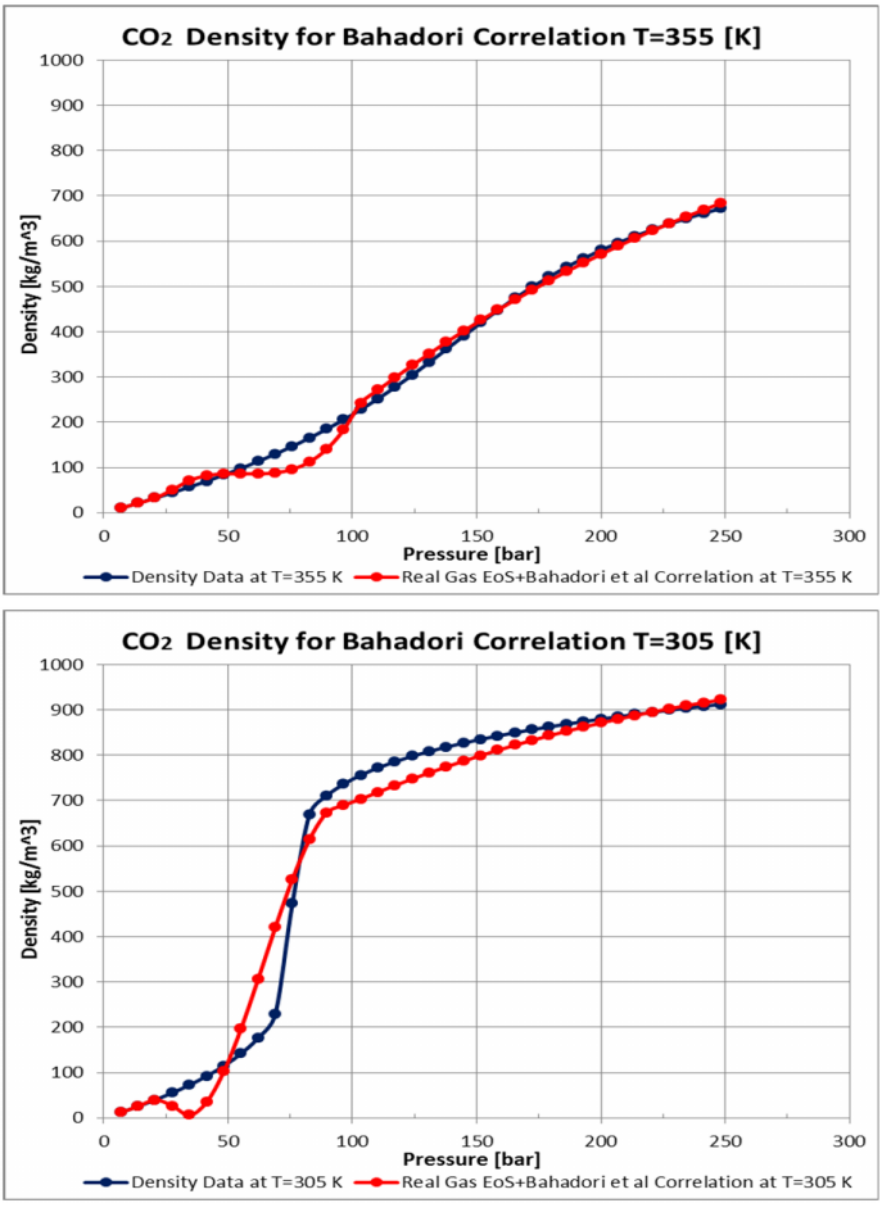

Figure 7 Predicting Carbon Dioxide density with Bahadori et al. Correlation

The prediction results by Bahadori et al. correlation and observed values [3] for T=305 [K] and T=355 [K] are shown in Figure 1. It is seen good performance to predict the density of carbon dioxide. Nevertheless, it seems to under predict values when used below 100 [bar] and for lower temperatures as in T= 305 [K]. As the density of carbon dioxide tends to exhibit a decreasing behavior with increase in temperature, the proposed equation shows good approximation Figure 7.

At low pressures, below 25 [bar], the behavior is modelled with real gas equation of state $PM = \rho zRT$, where the CO_2 is in gas phase and then the proposed correlation predicts the supercritical region. The blended equation is used in the extended version of ECLIPSE IDE UiS for Carbon Dioxide Injection. The AAE is 2.507 at T=305 [K] and 2.025 at T=355 [K].

B. Liang Biao Correlation

It is an explicit correlation to calculate density of carbon dioxide for conditions of a carbon capture and sequestration (CCS) project for the temperature range T= 313 [K] - 373 [K] and pressures between 75 [bar] and 620 [bar]. It can predict CO_2 density with very good matching to available carbon dioxide property data provided by the National Institute of Standards and Technology (NIST) web database [5] in which carbon dioxide properties have been generated for pressure and temperature ranges in CCS projects. It has been chosen due to great improvement over other few existing correlations such as Bahadori et al. [1].

The Liang Biao new correlation applies a least square approach and is associated to correlation coefficients that meet the criteria:

$$\sum \left(\rho_{pre} - \rho_{NIST}\right)^2 = \sum \left[\rho_{pre}(P,T) - \rho_{NIST}\right]^2 = \min imum \qquad \text{Equation 18}$$

ρ is carbon dioxide density in [kg/m^3]. The subscript "pre" refers to results for the proposed correlation and "NIST" refers to data value from NIST web database. The Liang Biao new correlation, as a function of pressure P in [psia], coefficients A_0 to A_4 function of temperature T in [^{0}C] and ρ density in [kg/m^3], is:

$$\rho = A_0 + A_1 P + A_2 P^2 + A_3 P^3 + A_4 P^4 \qquad \text{Equation 19}$$

$$A_i = b_{i0} + b_{i1} T + b_{i2} T^2 + b_{i3} T^3 + b_{i4} T^4 \qquad \text{Equation 20}$$

$$i = (0,1,2,3,4)$$

The values for correlation coefficients b_{i0} to b_{i4} (i=0, 1, 2, 3, 4) are given in Table 4 and Table 5.

Coefficient	b_{i0}	b_{i1}	b_{i2}	b_{i3}	b_{i4}
i=0	-2,15E+05	1,17E+04	-2,30E+02	1,97E+00	-6,18E-03
i=1	4,76E+02	-2,62E+01	5,22E-01	-4,49E-03	1,42E-05
i=2	-3,71E-01	2,07E-02	-4,17E-04	3,62E-06	-1,16E-08
i=3	1,23E-04	-6,93E-06	1,41E-07	-1,23E-09	3,95E-12
i=4	-1,47E-08	8,34E-10	-1,70E-11	1,50E-13	-4,84E-16

Table 4 Correlation coefficients for Liang Biao Correlation P ≤ 200 bar (Reference) [2]

Coefficient	b_{i0}	b_{i1}	b_{i2}	b_{i3}	b_{i4}
i=0	6,90E+02	2,73E+00	-2,25E-02	-4,65E-03	3,44E-05
i=1	2,21E-01	-6,55E-03	5,98E-05	2,27E-06	-1,89E-08
i=2	-5,12E-05	2,02E-06	-2,31E-08	-4,08E-10	3,89E-12
i=3	5,52E-09	-2,42E-10	3,12E-12	3,17E-14	-3,56E-16
i=4	-2,18E-13	1,01E-14	-1,41E-16	-8,96E-19	1,22E-20

Table 5 Tuned coefficients for Liang Biao Correlation P > 200 bar [2]

In his work Liang Biao cited "It can be clearly seen that at a particular temperature, carbon dioxide density increases with pressure. The higher the pressure, the higher the carbon dioxide density. And the lower the pressure, the lower the carbon dioxide density would be" [2]. Furthermore, the author found a perfect match to the NIST available data with his new developed correlation; this can also be seen for the present work compared to Reported Data [4] in Figure 8:

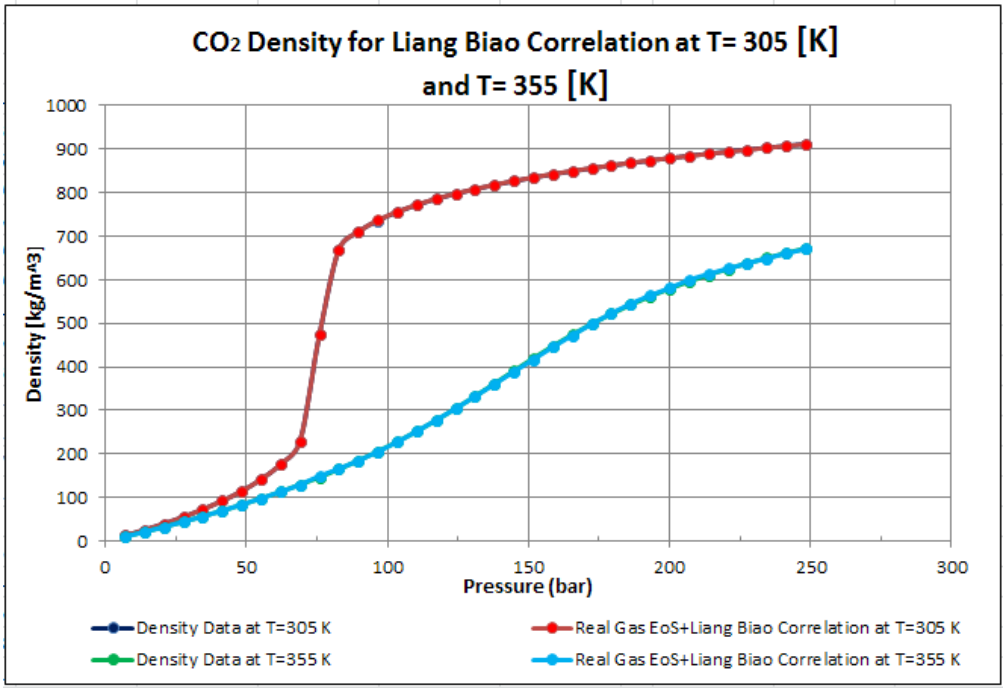

Figure 8 Predicting Carbon Dioxide density with Liang Biao Correlation

The real gas equation of state $PM = \rho zRT$ was used at low pressures (less than 75 [bar]). As the present work conditions are higher temperatures than the correlation temperature range of work, it was left to the real gas equation of state predicts the carbon dioxide density at the supercritical point (P=73.5 [bar]) and lower pressures for different temperatures considering "CO_2" at this condition as a "dense gas" as it is mentioned about Physical conditions of CO_2 in Section 2.8., this achieved well matching as it is seen in Figure 8. The AAE is -0.0355 at T=305 [K] and -0.1132 at T=355 [K].

2.8.1.2. Viscosity of Carbon Dioxide

For many years measurement of carbon dioxide viscosity has been subject of quite researches, most of them were reported in liquid phase, other in the vicinity of critical region and also in gas phase. Recently, special emphasis is given to the measurement and calculation of supercritical region in which carbon dioxide has been applied in purification processes and also for the present work in Enhance Gas Recovery EGR.

In literature, there are many references for predicting carbon dioxide viscosity such as Zabaloy et al. [6], Vesovic et al. [7], Fenghour et al. [8]. Unfortunately these correlations did not accurately predict carbon dioxide viscosity under supercritical conditions in which CO_2 injection will

operate. Moreover, those theoretical and empirical correlations need density or other thermodynamic parameters to calculate carbon dioxide viscosity. All the cited correlations ([6], [7], [8]) require temperature, density and knowledge of the fluid properties such as molecular weight, critical temperature and the critical pressure to estimate viscosity. Most of them correlate viscosity of pure supercritical fluids in a wide range of conditions and mainly for polar compounds. Nevertheless, when the mentioned correlations were tested for carbon dioxide and actual reservoir conditions, they were not sufficiently accurate. It has been necessary a correlation that can predict carbon dioxide viscosity under pressure and temperature changes.

It was chosen the most recent and updated viscosity correlation for pure carbon dioxide Heidaryan et al.

A. Heidaryan et al. Correlation

It is an explicit numerical correlation to calculate pure CO_2 viscosity at supercritical region based on new experimental data of current study using rolling-ball technique and reported data by Stephan and Lucas [9]. It was developed through multiple rational regression analysis to find an equation as a function of pressure and temperature which explains relationship between those variables.

The coefficients for Equation 22 were found to minimize the sum of residual squares SRS in Equation 21 are given in Table 6:

$$SRS = \sum_i \left(\mu_{\exp} - \mu_{cal}\right)^2 \qquad \text{Equation 21}$$

The subscript “exp” refers to experimental data of current study and “cal” refers to reported data by Stephan and Lucas. The proposed relation, which has more smooth ability to fit compared to a polynomial form, is expressed in Equation 10:

$$\mu = \frac{A_1 + A_2 P + A_3 P^2 + A_4 In(T) + A_5 (In(T))^2 + A_6 (In(T))^3}{1 + A_7 P + A_8 In(T) + A_9 (In(T))^2} \qquad \text{Equation 22}$$

In this correlation viscosity μ is in centipoise [cP], temperature T in Kelvin [K] and pressure P in bars [bar]. It is valid for pressure range from 75 [bar] and 1014 [bar] and temperature range from 305 [K] to 900 [K]; although it could be extended for other regions as the nonparametric regression exhibits CO_2 viscosity to be strong function of pressure and temperature.

Coefficients					
A_1	-0,1146067	**A_4**	0,0633612	**A_7**	6,51933E-06
A_2	6,97838E-07	**A_5**	-0,01166119	**A_8**	-0,3567559
A_3	3,97677E-10	**A_6**	0,00071426	**A_9**	0,03180473

Table 6 Coefficients for Heidaryan et al. Correlation [10]

For lower pressures than P=75 [bar], Lucas et al. (reference) and Lee at are used to predict carbon dioxide viscosity, then blended to the Heidaryan et al, it exhibits good consistency with the

proposed model at T=305 [K] in Figure 3; however, Lucas et al. is only valid for maximum temperature of T=305 [K]. The AAE 1.288 at T=305 [K] and 12.260 at T=355 [K] respectively. It shows a great error mainly because Lee et al., is commonly used for lighter gases and carbon dioxide even when it is in gas phase at those pressures, it is heavier gas, its results shows under prediction.

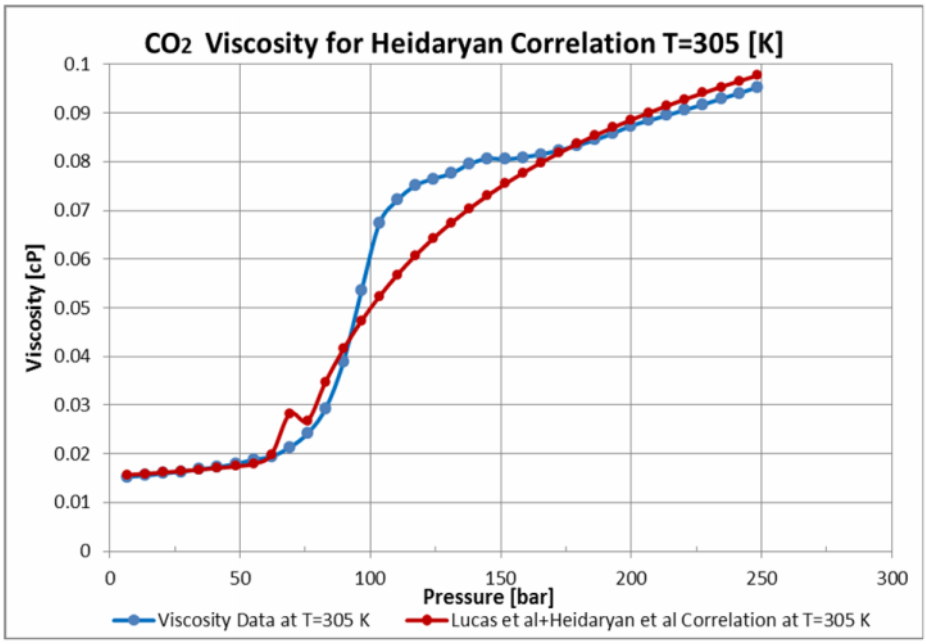

Figure 9 Results for Heidaryan et al. Correlation for T= 305 K and T= 355 K

2.9. Effects of Impurities on Geological Sequestration of Carbon Dioxide

Carbon dioxide sources can vary such as coal-fired power plants, refineries, gas plants, cement plants, then, CO_2 streams for injection and sequestration contain other components called "impurities" such as N_2, O_2, Ar, SO_x, NO_x, among others in different concentrations i.e., carbon dioxide for sequestration is not totally pure 100%; however, in this thesis, it is assumed a pure carbon dioxide stream for sequestration.

The recommended impurity limits are shown in Table 7 as the maximum amount of the component and the stream should be taken lower than the recommended levels except for carbon dioxide.

Those impurities can affect efficiency, safe transportation, storage systems with increased risk of corrosion or changes in the phase behavior of CO_2 stream for injection with respect to pure CO_2 stream. This could have important implications in the design and operation of the injection facilities from surface to reservoir.

Component	Concentration	Limitation
H_2O	500 ppm	Technical: below solubility limit of H_2O in CO_2 Cross effect of H_2O and CH_4 is significant but within limits for water solubility No significant cross effect of H_2O and H_2S
H_2S	200 ppm	Health and safety considerations
CO	2000 ppm	Health and safety considerations
O_2^*	EOR 100-1000 ppm	Technical: because lack of practical experiments on effects of O_2 underground
CH_4^*	EOR< 2 vol%	Energy consumption for compression and miscibility pressure for EOR
N_2^*	< 4 vol%	Energy consumption for compression
Ar^*	< 4 vol%	Energy consumption for compression
H_2^*	< 4 vol%	Further reduction of H_2 is recommended because of its energy content
SO_X	100 ppm	Health and safety considerations
NO_x	100 ppm	Health and safety considerations
CO_2	> 95.5%	Balanced with other compounds in CO_2

Table 7 DYNAMIS recommendation for CO_2 quality (Visser et al. 2009)
** The concentration limit of all non-condensable gases taken together, including O_2, CH_4, N_2, Ar, H_2 should not exceed 4 vol%* [11]

Particular aspects considered are:

- Potential effects of impurities on change in phase behavior and storage capacity calculations.
- Significant effects on injectivity through geochemical reactions in the vicinity of injection wells.
- Effects on buoyancy forces and trapping mechanisms.

Impurities from an oxyfuel combustion power plant could have components such as N_2, Ar, O_2, H_2O and maybe classified as condensable and non-condensable components, minor impurities as SO_2, SO_3, NO, NO_2, N_2, CO, and other micro-impurities which consists of HCl, HF, Hg and other heavy metals.

It can be considered three possible scenarios with regard to the level of CO_2 purity Table 8:

- Scenario 1: low purity option (CO_2 purity between 85%-90%)
- Scenario 2: medium purity option (CO_2 purity between 95%-98%)
- Scenario 3: high purity option (CO_2 purity greater than 99%)

Impurities on CO_2 injection stream can have physical and chemical effects into geological storage of carbon dioxide.

Component	Composition 1	Composition 2	Composition 3
CO_2 (vol %)	85.0	98.0	99.94
O_2 (vol %)	4.70	0.67	0.01
N_2 (vol %)	5.80	0.71	0.01
Ar (vol %)	4.47	0.59	0.01
H_2O (ppm)	100	100	100
NO_x (ppm)	100	100	100
SO_2, (ppm)	50	50	50
SO_3 (ppm)	20	20	20
CO(ppm)	50	50	50
Total	99.97%	99.97%	99.97%

Table 8 Composition of Oxy-fuel stream for CO_2 injection stream [11]

2.9.1. Physical Effects

It can be mentioned changes in physical properties such as density and phase. Due to the presence of non-condensable impurities such as N_2, O_2 and Ar, there are density changes and can also affect storage capacity and injectivity.

2.9.1.1. Effects on Phase Behavior

Non-condensable impurities can increase the bubble-point pressure and decrease critical temperature of pure CO_2 mostly because of their low critical temperature. It can be analyzed the greatest effect with the high impurity oxyfuel stream.

It is desired not to have two phase flow at all temperatures in the pipeline transportation of supercritical carbon dioxide and also in the injection facilities from surface to wellhead, wellhead to bottom hole and in the reservoir pore space.

If during transportation of supercritical CO_2, it has lower critical temperature, it will be required lower pipeline temperature and hence better cooling or insulation.

2.9.1.2. Effects on Storage Capacity

As it is discussed, density of CO_2 with other impurities affects not only CO_2 storage capacity but also buoyancy of the *CO_2 plume.*

The potential effect of non-condensable impurities is a reduction of CO_2 storage capacity, not only because of lower volume fraction of CO_2 in the stream but also mainly because they do not compress as high as pure CO_2 does. CO_2 storage capacity can be quantified for any CO_2 mixtures to see the impact of impurities:

$$\frac{M}{M_O} = \frac{\rho}{\rho_O\left(1+\sum\frac{m_i}{m_{CO2}}\right)}$$ Equation 23

M: mass of CO_2 in the mixture
M_0: mass of CO_2 in the pure stream
ρ: density of the mixture stream
ρ_0: density of pure CO_2 stream (zero impurity)
m_i/m_{CO2}: ratio of mass of impurity "i" to the mass of CO_2 in the mixture

M/M_0 the ratio of the mass of CO_2 per unit volume to that of pure stream could be named "normalized storage capacity" for carbon dioxide in its supercritical phase

The non-condensable impurities can greatly reduce density of carbon dioxide stream flowing in its supercritical state which reduces storage capacity compared to pure CO_2 stream as it is given a volume increase due to the volume fractions of those components. Considering different compositions of streams, a storage coefficient can be defined as:

$$E = \frac{G_{CO2}}{V_{CO2}\rho_{CO2}} \qquad \text{Equation 24}$$

E: storage coefficient
G_{CO2}: storage capacity in terms of CO_2 mass
V_{CO2}: total pore space available for CO_2 storage
ρ_{CO2}: carbon dioxide density

The storage capacity is in the basis of pure CO_2, taken into account the impurities in the CO_2 stream, storage capacity is lower. An impurity factor is introduced to estimate storage capacity for impure CO_2:

$$G_{CO2} = V_{CO2}\rho_{CO2}EF \qquad \text{Equation 25}$$

F: ratio of the CO_2 storage capacity in presence of impurities to that without presence of impurities. Numerically equal to the ratio M/M_0. Also called "impurity factor".

2.9.1.3. Effects on Buoyancy

Decrease in density of pure CO_2 created by the light-impurity components will cause increasing buoyancy. The buoyancy force of a mass of the plume in a unit volume in contact with formation water is:

$$F = \left(\rho_{H2O} - \rho_m\right)g \qquad \text{Equation 26}$$

Moreover, the effect of impurities (normalized buoyancy) on this force with respect to pure CO_2, neglecting capillary pressure and relative permeability, can be expressed as:

$$\frac{F}{F_O} = \frac{\rho_{H2O} - \rho_m}{\rho_{H2O} - \rho_{CO2}}$$ Equation 27

F: buoyancy force for the CO_2 mixture
F_0: buoyancy force for pure CO_2
ρ_{H2O}: densities of formation water
ρ_m: density of plume
ρ_{CO2}: density of pure CO_2

This greater density difference, as a consequence, would result in greater buoyancy which could reduce residual trapping of CO_2 into the geological formation. Moreover, this higher buoyancy of impure CO_2 streams will reduce carbon dioxide trapping in the rock pore spaces hence, CO_2 storage security underground could be reduced.

Furthermore, for pure CO_2 and CO_2 mixtures, because of the increasing density with higher pressures, the buoyancy force should decrease. Nevertheless, in previous equation relative buoyancy related to pure CO_2 increases with higher pressures, this is rewritten:

$$\frac{F}{F_O} = \frac{1 - \frac{\rho_m}{\rho_{H2O}}}{1 - \frac{\rho_{CO2}}{\rho_{H2O}}}$$ Equation 28

It can be noticed that pure CO_2 density increases with pressure more than the impure CO_2 density and this leads to the buoyancy ratio to increase with pressure.

2.9.1.4. Effects on Injectivity

The density change by non-condensable gas impurities leads to a lower injectivity of impure CO_2, as pressure increases, the injectivity could be almost equal to pure CO_2 because of decreased viscosity; the addition of impurities will cause such decrease. Nevertheless, more condensable gases such as SO_2 will have the effect of increasing injectivity because of increased density of CO_2 stream.

Non-condensable gases are less dense than CO_2 which significantly reduce density of supercritical CO_2 stream, and then it is related to that those impurities cause a volume increase.

Both the density and viscosity increase with pressure and decrease with temperature, the resultant injectivity does not change significantly with increasing depth. Moreover, relative injectivity is less sensitive to temperature at increasing depths; this is true as difference in density between pure and impure CO_2 decreases with increasing pressure and as difference in viscosity decreases with increasing temperature which is related to increasing depth.

CO_2 SEQUESTRATION IN GAS-CONDENSATE RESERVOIRS

CHAPTER 3

DISPLACEMENT MODELS FOR CARBON DIOXIDE INJECTION

In the aim of increasing natural energy of gas condensate reservoir for supplementary recovery of gas and liquids, it is necessary the injection of some fluid for displacing them towards producer wells. It was selected Carbon Dioxide as injection fluid because of its availability and increased popularity over the world to mitigate contribution of fossil fuel emissions, main contributor for climate change, reducing emissions to the atmosphere. Furthermore, it is found not to be miscible at reservoir conditions avoiding degradation of gas condensate quality due to great difference in properties between resident gas and injection fluid.

In this Thesis, it is assumed injection of pure CO_2 (mole fraction equal to 1 in injection stream), immiscible condition, carbon dioxide is in supercritical conditions from surface conditions (wellhead) to subsurface conditions (bottom-hole and reservoir) while reservoir depletion CO_2 can change into gas phase while reservoir temperature is invariable. The modelling of carbon dioxide properties takes into account this phase change to assure displacement process is valid for a wide range of pressure and temperature in the reservoir. CO_2 injected in well ICOGAS 1 will displace gas condensate towards production well PCOGAS 1.

For simulation of Carbon Dioxide Injection into a model gas condensate reservoir in which injection is to the pressure at a high level to minimize deposition and loss of retrograde liquid in the reservoir, it was constructed three different displacement models:

A. Gravity Segregation
B. Stable Displacement
C. Unstable Displacement

Those models are similar to a previous extension of the in-house simulator ECLIPSE IDE with dry gas injection. Therefore, the selection of displacement is based on angle of reservoir Θ, and flow injection rate of carbon dioxide q_{injCO2}.

3.1. Fundamentals of Displacement Models

The velocity of carbon dioxide flow and gas condensate flow is directly proportional to their mobilities as separated fluids. CO_2 will displace gas condensate in both ideal and non-ideal linear flow. It can be horizontal flow (Θ=0) and with a different geometry ($\Theta > 90^o$ or $\Theta = -90^o$).

The ideal linear flow occurs when mobility ratio M is lower than 1, it is a sharp interface between carbon dioxide 1and gas condensate, gas condensate will be flowing alone ahead of the interface and CO_2 will be flowing in the presence of some residual hydrocarbons behind the interface. It means gas condensate can be flowing with a velocity greater or equal to that of carbon dioxide. In this case, as CO_2 is displacing gas condensate, there will be no tendency for resident gas to be by-passed (fingering) which creates this sharp interface.

This is also called “piston-like displacement” from a linear reservoir in which total production of recoverable hydrocarbons (gas and liquid) are equal to the same volume of injection fluid. This is simulated in Chapter 4. From simulation results, it is observed that mobility ratio of the carbon dioxide injection will be in this range of $M \leq 1$.

The non-ideal linear flow occurs in the contrary if mobility ratio M is higher than 1. This indicates that carbon dioxide will be flowing faster than gas condensate and can create fingering, i.e., gas condensate will be by-passed. In the present Thesis, this was found when pressure is declining and viscosity value of carbon dioxide (injection fluid) change to gas phase and gets low values which make gas condensate travel faster into reservoir pore spaces. Therefore, higher injection fluid volume is necessary which can make the project be economically non-favorable.

3.2. Gravity Segregation Displacement for Carbon Dioxide Injection

This type of displacement is given mainly because of difference in density between fluids into the reservoir playing a role gravity forces. Due to great values of CO_2 density shown in Figure 5, it will be underrunning gas condensate. The bottom-hole injection pressure which is smoothly higher than reservoir pressure makes gas condensate will travel upwards while carbon dioxide downwards. Carbon dioxide can try to travel towards injection well but favorable because gas condensate to flow towards production well.

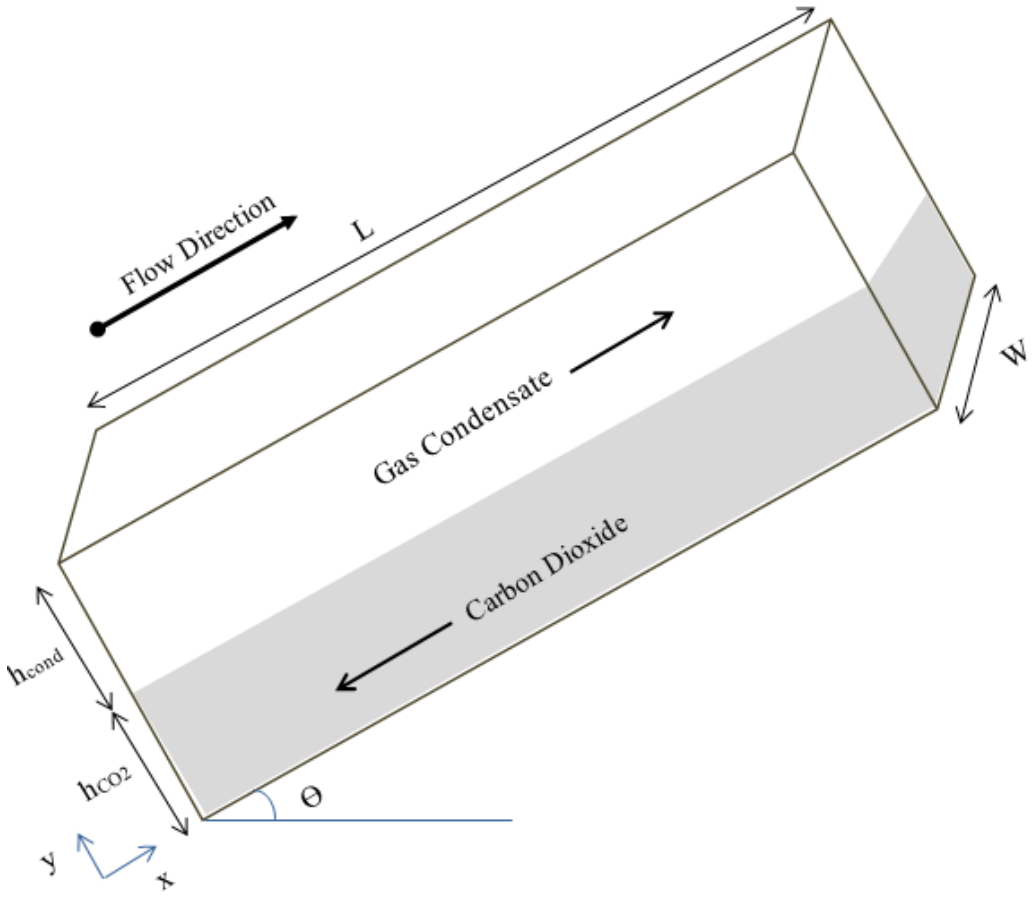

Figure 10 Scheme of Gravity Segregation Displacement for Carbon Dioxide Injection

This displacement as seen in Figure 10 Scheme of Gravity Segregation Displacement for Carbon Dioxide Injection in which reservoir is inclined upward, positive inclination Θ.

Furthermore, carbon dioxide injection rate q_{injCO2} must be lower than the maximum CO_2 injection rate in order not to change to stable displacement. In this case, injection rate is equivalent to injection pressure such that bottom-hole injection pressure does not exceed reservoir pressure.

Derivations of flow equations and pressure drop into Gravity Segregation Displacement for carbon dioxide are in Appendix 1.

The maximum injection rate that can be before to change to Stable Displacement is:

$$q_{\max .CO2} = \frac{k_{CO2}}{\mu_{CO2}}\left(\rho_{CO2} - \rho_{cond}\right) g \sin\theta \frac{Wh}{\left(1+\sqrt{M}\right)^2} \qquad \text{Equation 29}$$

This is the limit injection rate for carbon dioxide in the gravity segregation condition. The total pressure drop is found from Darcy´s Law studied in Section 1.

Pressure drop in gas condensate:

$$\Delta P_{cond} = -\left(\frac{q\mu_{cond}}{kWh_{cond}} + \rho_{cond} g \sin\theta\right) L \qquad \text{Equation 30}$$

Pressure drop in Carbon Dioxide:

$$\Delta P_{CO2} = -\left(\frac{q\mu_{CO2}}{kWh_{CO2}} - \rho_{CO2} g \sin\theta\right) L \qquad \text{Equation 31}$$

Finally, total pressure drop:

$$\Delta P_{total} = \Delta P_{cond} + \Delta P_{CO2}$$

$$\Delta P_{total} = -\left[\frac{q}{KW}\left(\frac{\mu_{cond}}{h_{cond}} + \frac{\mu_{CO2}}{h_{CO2}}\right) - \left(\rho_{CO2} - \rho_{cond}\right) g \sin\theta\right] L \qquad \text{Equation 32}$$

3.3. Stable Displacement for Carbon Dioxide Injection

In this type of displacement, it is assumed an ideal flow, piston displacement, in which displacement front travels parallel to the direction of flow. Gas condensate is flowing alone ahead displacement front while gas condensate that is being injected flows behind front displacement. Reservoir inclination is negative, downward inclined reservoir.

The density difference between both fluids: resident gas and injection fluid is still important. Moreover, angle between the interface of both fluids and flow direction remains constant through this displacement.

$$\frac{dy}{dx} = -\tan\beta = cons\tan t$$

Besides the other features, it is observed that this type of displacement is achieved at low injection rates, then, gravity forces given by density difference between fluids is trying to maintain displacement front horizontal, meaning stable Figure 11.

When given high injection rates, viscous forces, those which drive carbon dioxide and gas condensate through reservoir, can be greater than gravity forces which can result in an unstable displacement.

When incompressible flow displacement is stable, all points on the interface have the same velocity at any point on that interface.

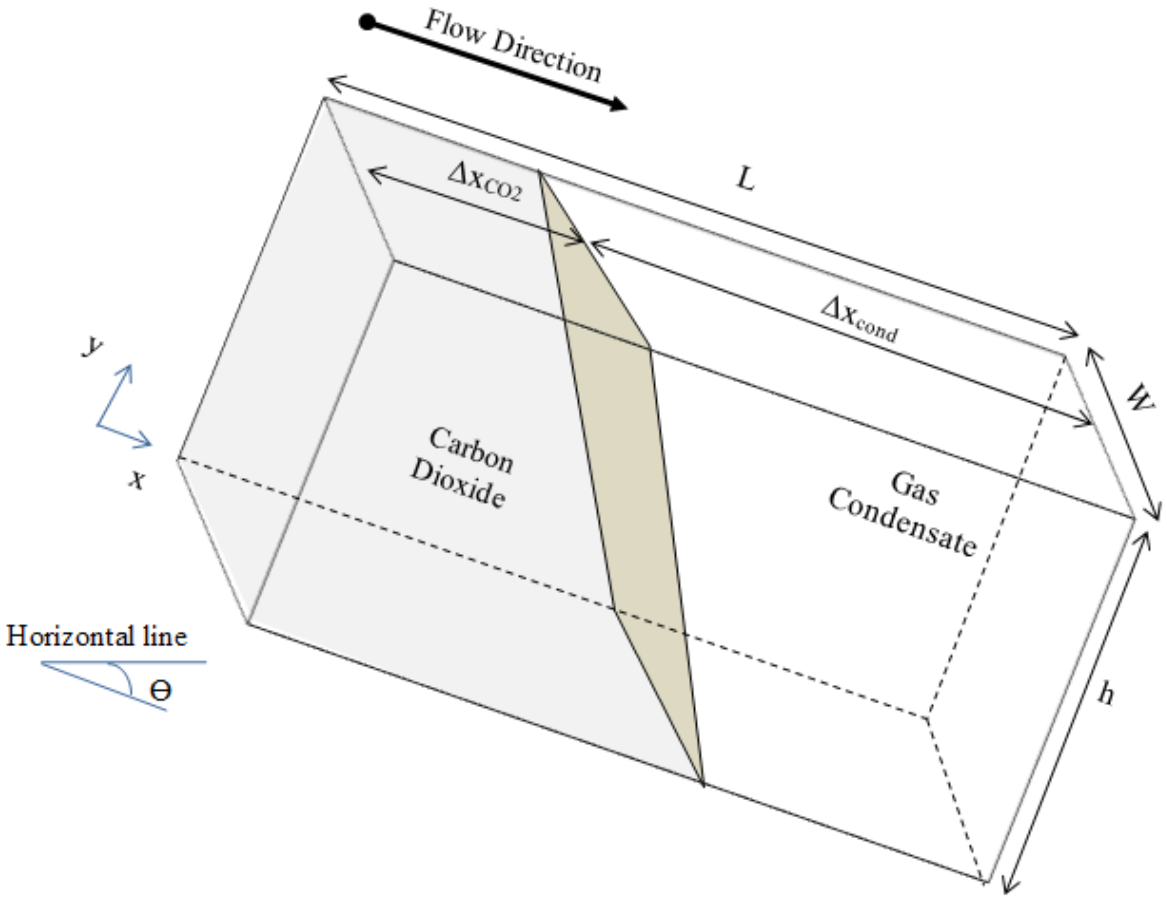

Figure 11 Scheme of Stable Displacement for Carbon Dioxide Injection

All flow equations and pressure derivation are found applying Darcy´s Law in Appendix 2.

There is a critical injection rate $q_{critCO2}$ for carbon dioxide to underrun gas condensate.

$$q_{critCO2} = 8.64E-8\frac{k_{CO2}}{\mu_{CO2}}A\frac{\Delta\rho g\sin\theta}{(M-1)}$$ Equation 33

CO_2 injection rate q_{injCO2} must be maintained below this critical rate such that gravity forces stabilizes the displacement and maintains the front displacement like a well-defined interface that travels parallel to the horizontal line.

Pressure drop for gas condensate and carbon dioxide:

$$\Delta P_{cond} = -\left(\frac{q_{cond}\mu_{cond}}{kA} - \rho_{cond} g\sin\theta\right)\Delta x_{cond}$$ Equation 34

$$\Delta P_{CO2} = -\left(\frac{q_{CO2}\mu_{CO2}}{kA} - \rho_{CO2} g\sin\theta\right)\left(L - \Delta x_{cond}\right)$$ Equation 35

It can also be grouped to identify the term $\Delta\rho = \left(\rho_{CO2} - \rho_{cond}\right)$ and the term $\left(\Delta\rho\Delta x_{cond} - \rho_{CO2} L\right)g\sin\theta$ that accounts for the gravity term of the equation.

$$\Delta P_{total} = -\left[\left(\frac{q_{cond}\mu_{cond}}{kA}\Delta x_{cond} + \frac{q_{CO2}\mu_{CO2}}{kA}\left(L - \Delta x_{cond}\right)\right) + \left(\Delta\rho\Delta x_{cond} - \rho_{CO2} L\right)g\sin\theta\right]$$ Equation 36

3.4. Unstable Displacement for Carbon Dioxide Injection

When a less viscous injection fluid is displacing a more viscous fluid, the displacement front becomes unstable, like fingers, and can grow due to variation of reservoir permeability in which fluid can travel or fast or slow through pore spaces into the reservoir, this phenomenon known as viscous fingering.

When injection rate of carbon dioxide q_{injCO2} is higher than critical rate $q_{critCO2}$, this type of displacement is created, front displacement is not stable.

Those equations that govern displacement of both fluids are Darcy´s Law and mass conservation for both phases in which carbon dioxide is still considered a dense gas as discussed in Chapter 2.

The assumed scheme for carbon dioxide in viscous fingering displacement is shown in Figure 12 where CO_2 is underrunning gas condensate due to higher density in comparison to the gas condensate.

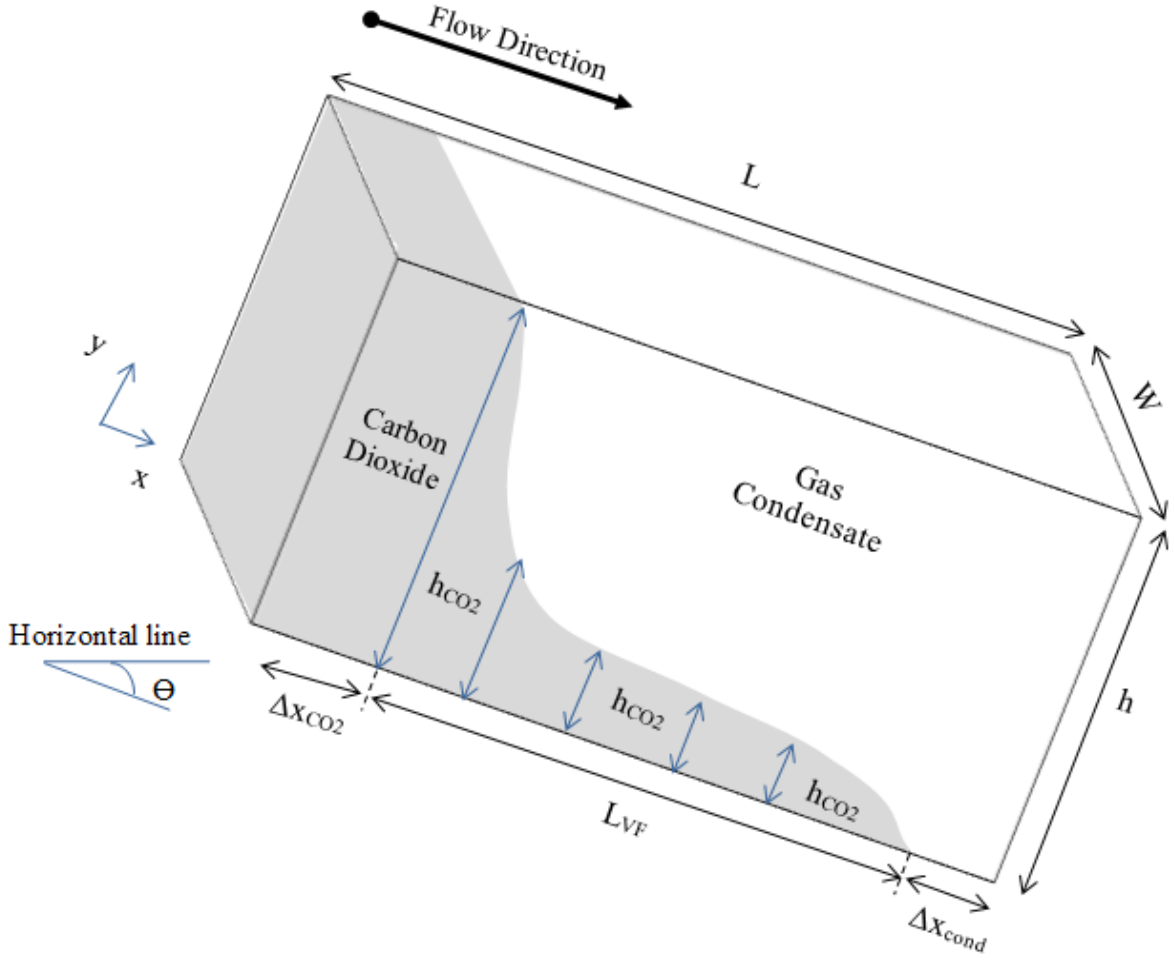

Figure 12 Scheme of Unstable Displacement for Carbon Dioxide Injection

In Figure 13 it is observed the saturation profile for carbon dioxide, the end of front displacement when saturation S is zero and at the rear of front displacement saturation S is one. A viscous fingering zone is created when carbon dioxide flows faster than gas condensate for values of mobility ratio greater than 1. Behind and ahead this region carbon dioxide and gas condensate will be flowing alone, gas condensate towards to production well and CO_2 from injection well displacing resident gas towards production well.

The length of this viscous fingering zone is important to know:

$$L_{VF} = x_f - x_r = \frac{q_{total}\, t}{\phi W h}\left(M - \frac{1}{M}\right) \qquad \text{Equation 37}$$

Flow pressure drop for carbon dioxide, viscous fingering region, gas condensate respectively are completely described in Appendix 3:

$$\Delta P_{CO2} = -\frac{q_{CO2}}{A}\frac{\mu_{CO2}}{k_{CO2}}\Delta x_{CO2}$$ Equation 38

$$\Delta P_{VF} = -\frac{2}{3}\frac{q_{total}^{2}t}{\phi(Wh)^2}\frac{\mu_{cond}}{k_{cond}}\frac{(M^2-1)^{3/2}}{M^2}$$ Equation 39

$$\Delta P_{cond} = -\frac{q_{cond}}{A}\frac{\mu_{cond}}{k_{cond}}\left(L - \Delta x_{CO2} - L_{VF}\right)$$ Equation 40

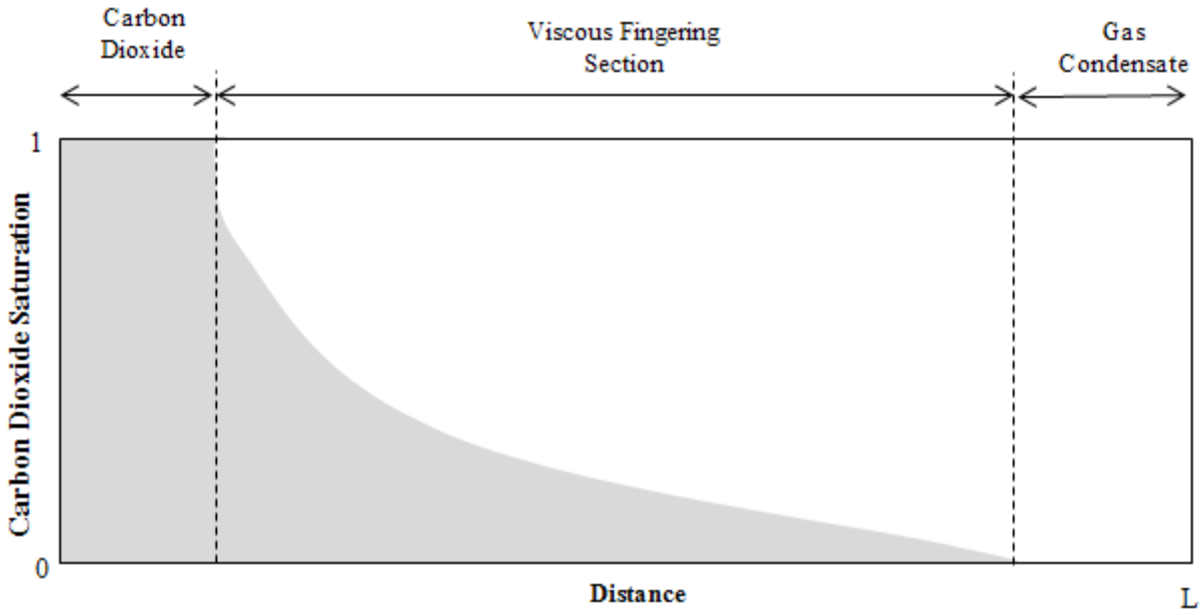

Figure 13 Saturation of Carbon Dioxide as a function of distance in Injection Displacement

CO_2 SEQUESTRATION IN GAS-CONDENSATE RESERVOIRS

CHAPTER 4

SIMULATION METHODS

For the present Thesis, ECLIPSE IDE UiS, in-house simulator was used. This is a Natural Gas Reservoir Simulator capable of simulating natural depletion (material balance), extension with multi well option, with gas (re)injection (material balance) and with simulation of displacement mechanisms in (re) injection process.

It was implemented a new extension with simulation of displacement mechanisms for carbon dioxide injection process. For this, the NGASSIM-program was updated with new subroutines to include investigation of flow pressure drop for CO_2 for different type of displacements, modelling of carbon dioxide properties and wellhead and bottom-hole pressure for injector well.

The new version incorporates 3 different displacement models Gravity Segregation, Stable and Unstable Displacement for CO_2 Injection, also calculates carbon dioxide properties: *density* by means of Bahadori et al. and Liang Biao correlations and *viscosity* by means of Heidaryan et al. correlation.

4.1. Overview of Simulation Program

The simulation program has a Main Program which calls to different subroutines to perform different calculations to simulate current process of natural gas reservoirs.

The Main Program has three processes to be run. First, a procedure to initialize it with three different data files:

A. NGASDATA.DAT
B. NGASLOG.DAT
C. NGASPRNT.DAT

In the NGASDATA.DAT, it is specified all input information for the program to carry out the simulation. In the NGASLOG.DAT is written all information that has been read from the previous file. Moreover, a summary from calculations done in the simulation are found in this file. The NGASPRNT.DAT shows the results of all calculations from current simulation that has been run; also error messages can be seen in this file if the program has found some error when running.

There are three fundamental subroutines for the Main Program:

a. GASPROD
b. READDATA
c. WRITEDATA

The first *GASPROD* subroutine organizes all simulation process to be run, initializes input data, defines main time step loop, updates variables, prints data to log file to do this other programs are called from GASPROD subroutine such as: PVTTAB, MATRBAL among others and also the new created subroutines.

The second *READDATA* subroutine reads all data contained in the NGASDATA.DAT (data file), after that, returns to the main program to call the third *WRITEDATA* subroutine that writes all necessary data to NGASLOG.DAT (log file).

To carry out simulation process is included an initialization procedure in which are defined all needed parameters used in the program, a CPU clock is started and stopped, and the simulation results are recorded and transferred to the main program as different output data files with extension .CSV.

Specification	**FILES**	**SUBROUTINES**	**OUTPUT Data Files**
Data File	NGASDAT.DAT	READDATA	NGASPROD.CSV
Log File	NGASLOG.DAT	WRITEDATA	NGASPBLK.CSV
Print data file	NGASPRNT.DAT	GASPROD	NGASWPRD.CSV
		MATRBAL	NGASP-WG.CSV
		INFLOW	NGASP-BH.CSV
		WHPRESS	NGASP-WH.CSV
		PRODRATE	NGASWRAT.CSV
		INJFLOW	INJWRAT.CSV
		INWHPRESS	NGINJ-BH.CSV
		INCDWHPRESS	NGINJ-WH.CSV
		INPDROP	MODVF.CSV
		INJCDPDROP	PDIN.CSV
	Other Subroutines	AQINFLUX	DISPCD.CSV
		GASFAC	INJCDPDROP.CSV
		PVTTAB	
		REED	
		GASCOMPR	
		LEEVISC	
		ZFACTOR	
		HEYVISC	
		LIANGDEN	
		BAHDEN	

Table 9 Simulation Program Overview

4.2. Implementation of New Subroutine INJCDPDROP

The main program has been extended to simulate displacement mechanisms of carbon dioxide injection into the example gas condensate reservoir currently being studied. It was updated with the subroutine named INJCDPDROP which calculates pressure drop in reservoir due to carbon dioxide injection. It is in color dark gray in Table 9.

The main concern related to high injection rate of carbon dioxide for pressure maintenance was solved with calculation of bottom hole injection pressure and wellhead injection pressure for injector well ICOGAS 1. Furthermore, it can be also seen when CO_2 breakthrough takes place and how carbon dioxide flows in the reservoir. To do so, this subroutine incorporates 3 different displacement models: Gravity Segregation, Stable and Unstable Displacement in a similar way as the extension of injection of dry gas INPDROP.

Through all program the letters CD stands for Carbon Dioxide (injection fluid) and GC for gas condensate (resident gas).

Moreover, to carry out simulation of carbon dioxide, it was necessary to model the 2 most important carbon dioxide properties for injection process: *density and viscosity.* For density, it was implemented the programs LIANGDEN and BAHDEN, both of them can be used in simulation, the Liang Biao correlation and Bahadori et al correlation are used respectively. For viscosity, it was necessary the program HEYVISC with Heydaryan et al correlation. Those are in light grey in Table 9. They are described in Chapter 2. Also, it can be seen in Figure 5 and 6, the results of those correlations at reservoir conditions for injection rate of 3E5 [Sm^3/day], injection starts at time t= 100 day and stops at time t=500 day.

4.3. Description of Subroutine INJCDPDROP

The new program calls to the subroutine PVTTAB before calculating density and viscosity of CO_2 and gas condensate which is necessary for the program. The compressibility z factor at bottom-hole conditions needed for the subroutine INCDWHPRESS is taken equal as the z factor provided in the PVT Table for the current lab data described in NGASDATA.DAT file (Appendix 4).

In the program, the bottom-hole injection pressure is a mean between average reservoir pressure and total pressure drop such that does not exceed initial reservoir pressure. If there is no injection of carbon dioxide, wellhead injection pressure is zero; when it is being injected the subroutine INCDWHPRESS was also implemented to calculate the wellhead pressure for injection well; it is function of wellbore pressure drop and bottom-hole injection process and exceeds it.

When injection stops, the wellhead injection pressure is a summation of bottom-hole injection pressure and static wellbore pressure drop. The bottom-hole injection pressure then gets the value of reservoir pressure (pressure in block).

Then, it is calculated the maximum q_{max} and critical q_{crit} injection flow rate to determine which displacement process takes place joined to the input data file referred to angle of reservoir inclination comparing those values to the carbon dioxide injection rate q_{injCO2}.

Next, according to the given conditions, the current displacement calculates carbon dioxide and gas condensate lengths if gravity segregation or stable displacement and/or viscous fingering length if unstable displacement which are function of time and according to the position of observation.

Finally, the results from simulation are given in the output data files named: DISPCD.CSV and INJCDPDROP which are in light grey in Table 9.

4.4. Simulation Model

The injector well ICOGAS 1 has an extension of about 300 [m] in x direction and 100 [m] in y direction. The thickness is about 50 [m]. The reservoir depth is 3500 [m]. The Gas Initially In Place (GIIP) is 0.8763 billion [m^3] and Liquid Initially in Place (LIIP) is 0.4175 million [m^3]. The Initial Reservoir Pressure was 437 [bar] and Reservoir Temperature is 392 [K]. The standard conditions are Standard Pressure of 1.01 [bar] and Standard Temperature of 288 [K].

It is described in the following paragraphs different scenarios of CO_2 Injection. The strategy is to see the effects in changing flow injection rate for the different displacement models. The example gas well described in Table 10 and Table 11 is not in order to decide about an optimum strategy for gas condensate reservoirs; in contrast whilst is to analyze general effects of injection of carbon dioxide on this as a typical example of a retrograde gas reservoir.

Reservoir Characteristics		
V_p= 4 000 000 [Rm^3]	S_w= 0.2	P_i= 437 [bar]
r_e= 350 [m]	k= 100 [mD]	T_i= 392 [K]
h= 50 [m]	C_A= 31.62	c_w= 4.35 x 10^{-5} [1/bar]
ϕ= 0.2	S= 0	c_R= 4. 5 x 10^{-5} [1/bar]

Table 10 Reservoir Characteristics of the Example Gas Condensate Field

Wellbore Characteristics	
Well= ICOGAS 1	Well= PCOGAS 1
Type= Injector	Type= Producer
r_w= 0.274 [m]	r_w= 0.175 [m]
H= 3500 [m]	H= 3500 [m]
T_{WH}= 313 [K]	T_{WH}= 313 [K]
S= 0	S= 0
Tubing Data	Tubing Data
ID= 0.2 [m]	ID= 0.2 [m]
ε= 1.5 E-5 [m]	ε= 1.5 E-5 [m]
α= 0^0	α=0^0

Table 11 Wellbore Characteristics of the Example Gas Condensate Field

The Case 1 is named Base Case, natural depletion of the PCOGAS 1 well, there is no injection. Case 2 refers to different flow injection rate of carbon dioxide for Gravity Segregation Model. Case 3 and Case 4 is referred to different carbon dioxide injection rate for Stable and Unstable Displacement Model respectively.

4.4.1. CASE 1: Base Case Natural Depletion

For this simulation, the reservoir is producing without injection of any fluid, it can be seen how gas production rate is decreasing fast as the reservoir is being depleted. The cumulative gas recovery of 0.8108 billion [m^3] and liquid recovery of 0.2996 million [m^3]. The final reservoir pressure is 30.1 [bar].

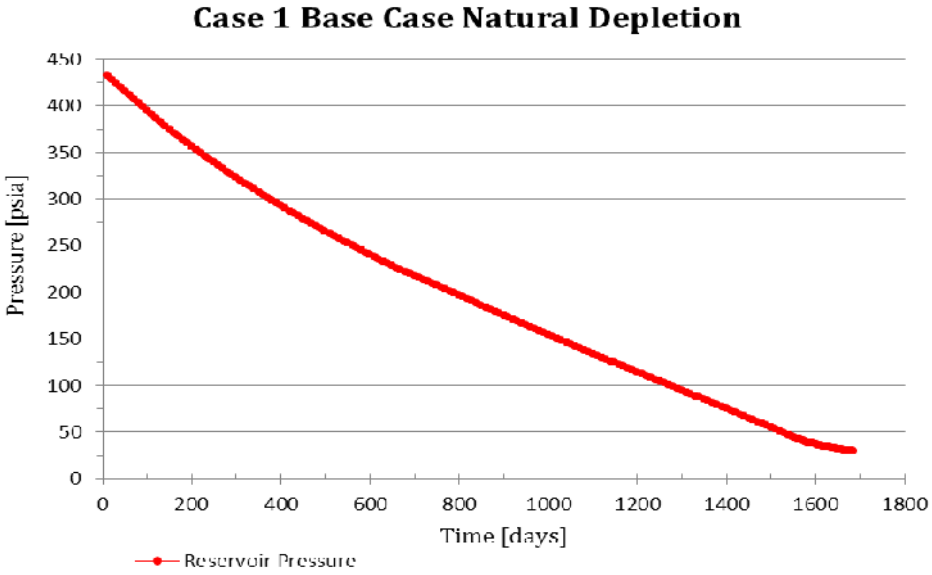

Figure 14 Reservoir Pressure for Case 1 Base Case Natural Depletion

4.4.2. CASE 2: Carbon dioxide injection rate= 2 E5 [Sm3/day] for Gravity Segregation Displacement

The flow injection rate of carbon dioxide was chosen such that it can help to increase reservoir pressure and economically viable, those selected were: 3E5 [Sm^3/day] and 5E5 [Sm^3/day], this last is equal to the amount of gas being produced i.e., gas rate of 5E5 [Sm^3/day].

In this case, carbon dioxide injection rate must be lower than the maximum flow injection rate for gravity segregation named "q_{maxCO2}" this was selected to be 2 E5 [Sm^3/day] Furthermore, the reservoir must be inclined upward. The injection duration is of 400 days, start of injection at time T= 100 day and stop time at time T=500 day.

For the total pressure drop, this is dominated by the gravitational effect more than viscous effect due to high values of carbon dioxide density; a higher pressure drop in carbon dioxide section than in gas condensate section. It is given a cumulative gas production of 0.8587 million [Sm^3/day] and liquid production of 0.3237 million [Sm^3/day]. The final reservoir pressure is 42.6 [bar].

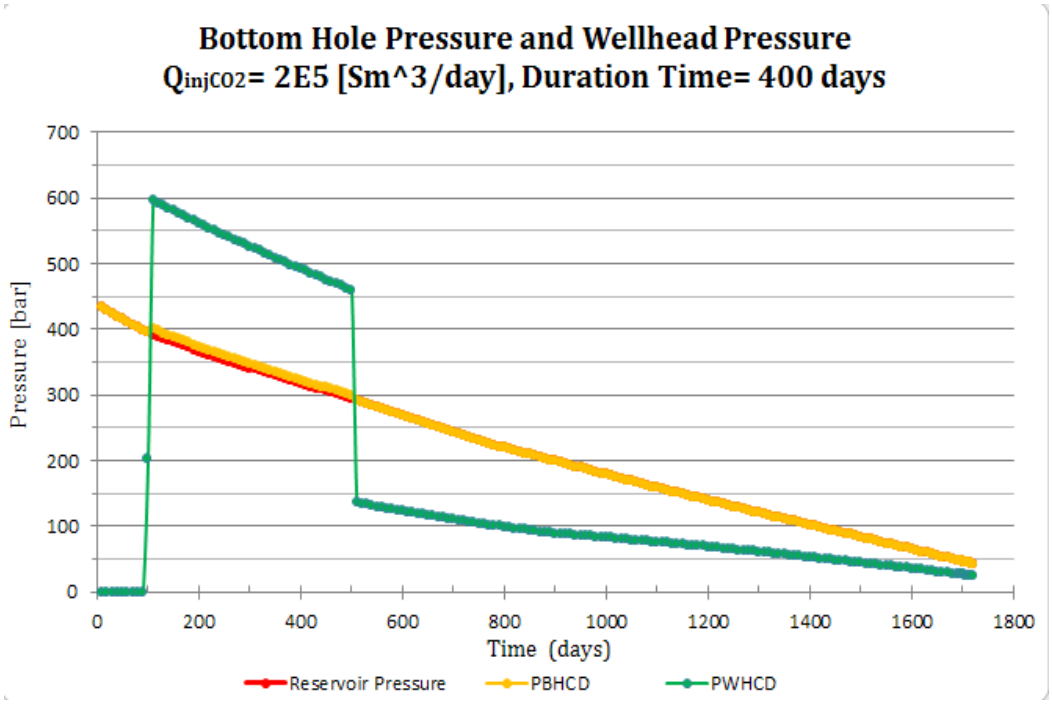

Figure 15 Carbon Dioxide Injection Rate of 2 E5 [Sm3/day] for Gravity Segregation Model; Θ= 45 degrees; Start of Injection= 100 day; Stop of Injection= 500 day

4.4.3. CASE 3: Carbon dioxide injection rate= 1 E4 [Sm3/day] for Stable Displacement

For stable displacement, the reservoir is inclined downwards i.e., down dip reservoir also, carbon dioxide injection rate is lower than critical flow rate "$q_{critCO2}$", in the contrary, unstable displacement takes place.

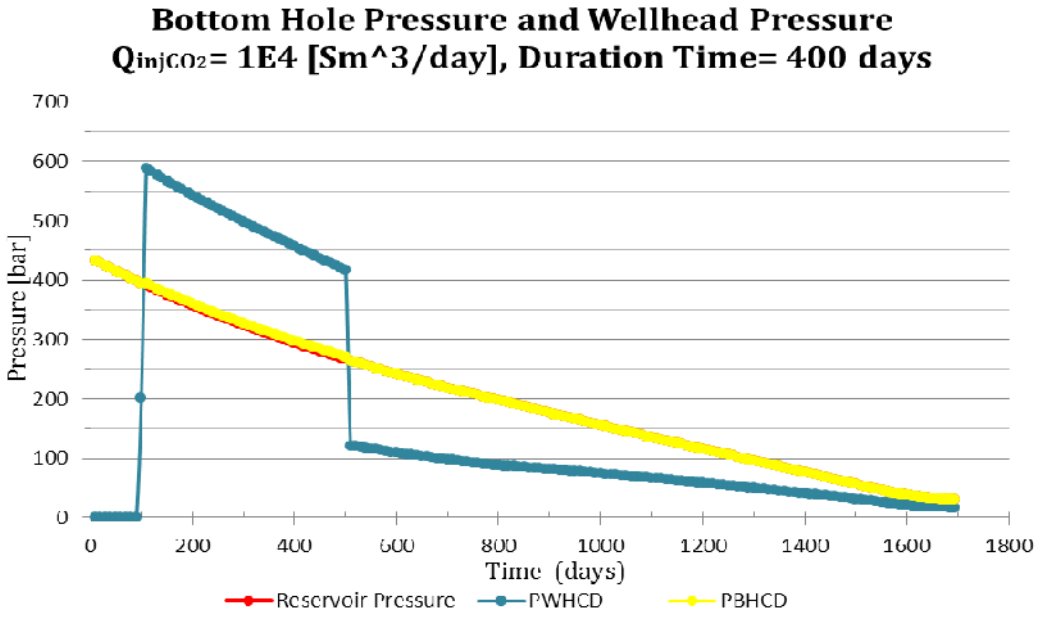

Figure 16 Carbon Dioxide Injection Rate of 1 E4 [Sm3/day] for Stable Displacement; Θ= - 30 degrees; Start of Injection= 100 day; Stop of Injection= 500 day

The final reservoir pressure is 30 [bar], injection rate is very low in comparison the selected injection flow rate of 3 E5 [Sm^3/day] to 5 E5 [Sm^3/day] consequently, pore spaces are not being replaced by carbon dioxide and reservoir pressure is being similarly depleted.

Moreover, the total flow pressure drop has a positive value, pressure drop in gas condensate region is positive, mobility ratio is favorable to gas condensate then it travels faster than carbon dioxide which results in a positive difference of (Lobs-Δx_{CO2}) that makes the value of ΔP_{cond} dominates the total pressure drop while ΔP_{CO2} is negative, gravitational effects are greater than viscous effects; high value of carbon dioxide density contributes into a great extent to the pressure drop in carbon dioxide region. Moreover, mobility ratio is less than 1 as long as carbon dioxide viscosity is more viscous than gas condensate, next, it moves slower when displacement takes place into reservoir, injection fluid is under supercritical state as reservoir conditions states suitable conditions above its critical pressure and critical temperature, carbon dioxide is considered as a gas dense.

$\Delta P_{FLOW} = \Delta P_{cond} + \Delta P_{CO2}$

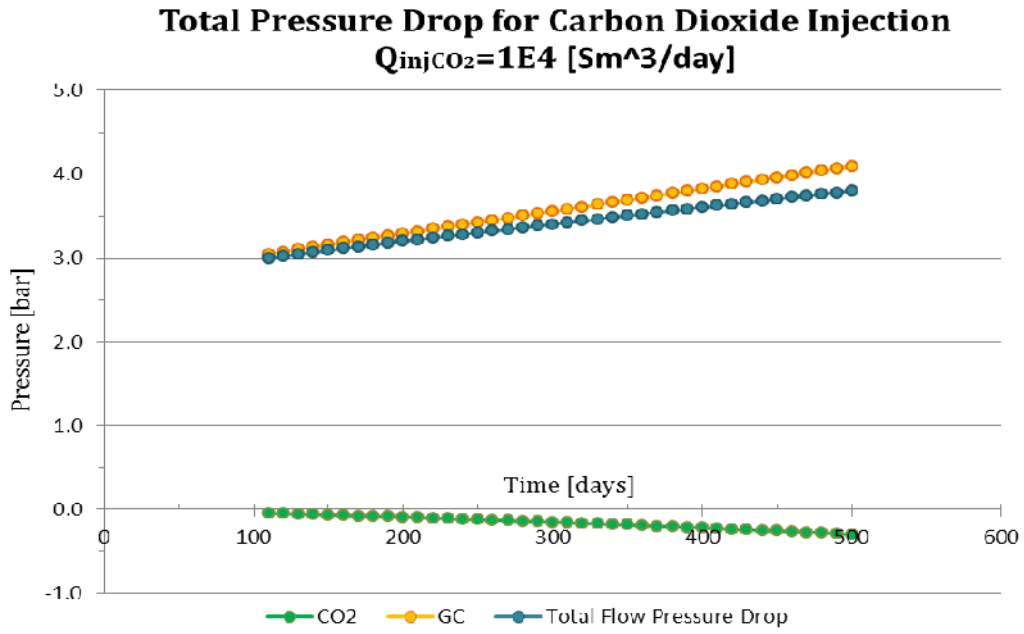

Figure 17 Total Pressure Drop for Carbon Dioxide Injection in Stable Displacement Q_{inj}= 1E4 [Sm^3/day] and Θ= -30 degrees

4.4.4. CASE 4: Carbon dioxide injection rate= 3E5 [Sm3/day] for Unstable Displacement

Carbon dioxide injection rate was chosen such that bottom-hole pressure does not exceed initial reservoir pressure in any moment of injection while trying to maximize injected CO_2 amounts. The cumulative amount of gas produced and liquid produced when injection rate of carbon dioxide equal to 3E5 [Sm^3/day] for an injection time of 400 days is 0.8546 million [Sm^3/day] and 0.3281 million [Sm^3/day] respectively.

Start of injection at t=100 day was found suitable in order to increase reservoir pressure and not to fall quickly into retrograde region where liquid entrapment into pores occurs that makes those liquids are not being produced. Simulations start with this time and stop at different injection time and develop different scenarios.

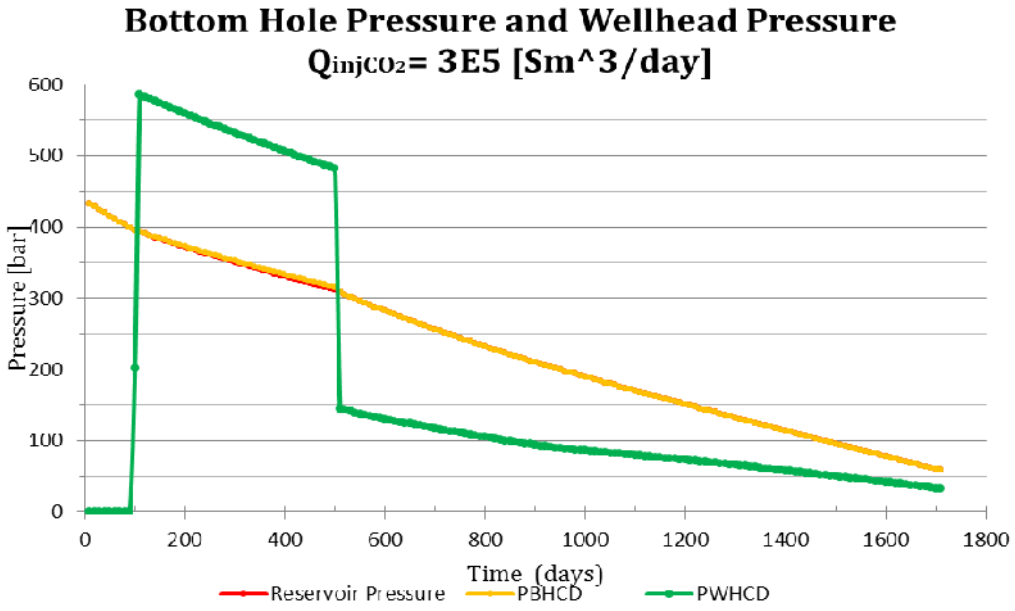

Figure 18 Carbon Dioxide Injection Rate of 3 E5 [Sm3/day] for Unstable Model; Start of Injection= 100 day; Stop of Injection= 500 day Injection Time: 400 days

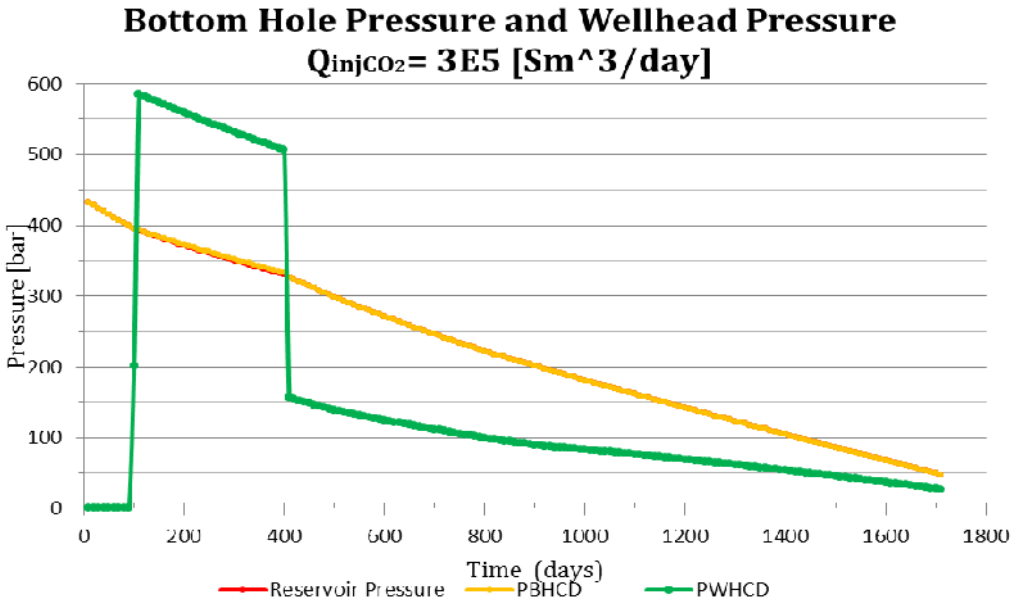

Figure 19 Carbon Dioxide Injection Rate of 3 E5 [Sm3/day] for Unstable Model; Start of Injection= 100 day; Stop of Injection= 400 day Injection Time: 300 days

In order to avoid too high pressures; bottom-hole injection pressure to be above initial reservoir pressure; it is not advisable to inject early in the lifetime but in the aim of pressure maintenance; not late to retard the time to fall into the retrograde region.

In Figure 18 and Figure 19 are simulated for an injection rate of 3E5 [Sm^3/day] different injection times. None of them exceeds initial reservoir pressure for bottom hole injection pressure. It is observed better pressure maintenance effect for injection time of 400 days with a final reservoir pressure of 58.2 [bar] in comparison to 47.7 [bar] for injection time of 300 days. There is no breakthrough of carbon dioxide.

In Figure 20 it is seen simulation of a carbon dioxide injection rate of 3E5 [Sm^3/day] starting at a time t=100 days for a duration of 700 days. It was found even a better pressure maintenance than the two previous cases with a final reservoir pressure of 87 [bar]. Also, bottom hole injection pressure is not above initial reservoir pressure; reservoir conditions are given such that carbon dioxide does not experiment phase change from supercritical conditions compared to the previous cases when CO_2 could change to gas phase given reservoir conditions.

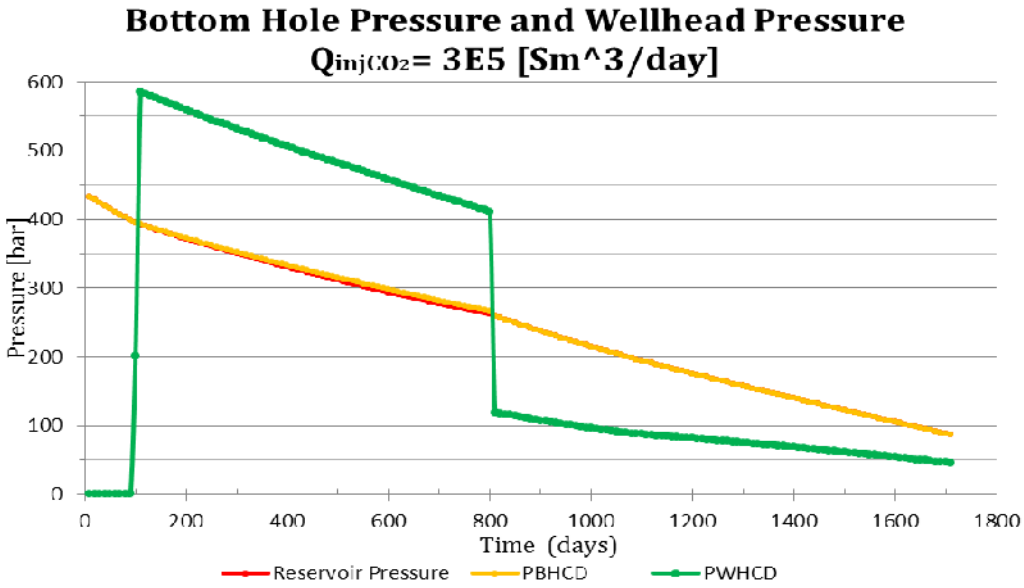

Figure 20 Carbon Dioxide Injection Rate of 3 E5 [Sm3/day] for Unstable Model;
Start of Injection= 100 day; Stop of Injection= 800 day
Injection Time: 700 days

The total gas production and liquid production of 0.8546 billion [m^3] and liquid recovery of 0.3382 million [m^3]. Nevertheless, it is expected breakthrough of carbon dioxide at time t=550 day Figure 21.

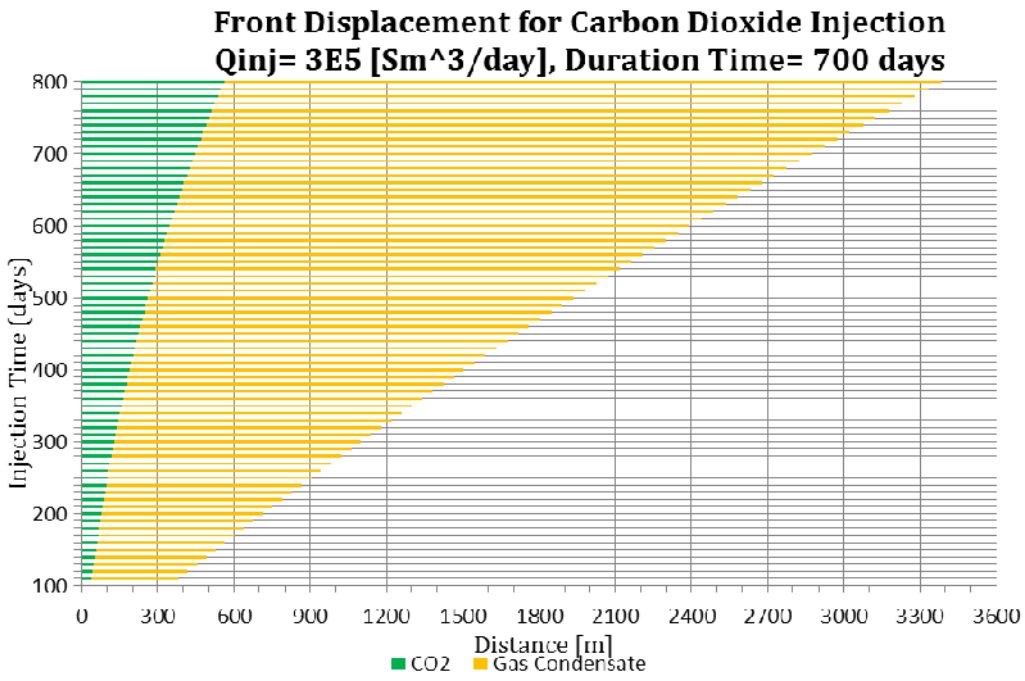

Figure 21 Front Displacement for Carbon Dioxide Injection in Unstable Model; Start of Injection= 100 day; Stop of Injection= 800 day

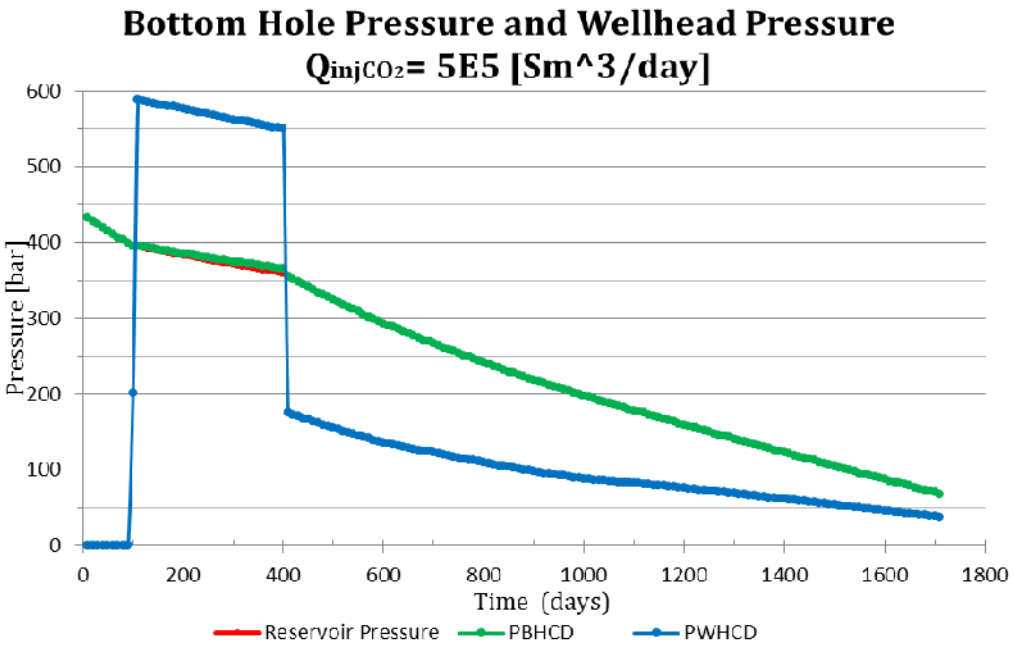

Figure 22 Carbon Dioxide Injection Rate of 5 E5 [Sm3/day] for Unstable Model; Start of Injection= 100 day; Stop of Injection= 400 day Injection Time: 300 days

Another option to select flow injection rate is such that carbon dioxide injection rate to be equal to gas production rate. In such case, it is given a gas rate of 5 E5 [Sm^3/day]. In Figure 22, for an

injection time of 300 days, carbon dioxide does not cause breakthrough; at the end reservoir pressure is 67.9 [bar], the highest well head injection pressure in well ICOGAS 1 to be 589 [bar]. An increment in liquid production of 0.3328 million [m^3] compared to 0.3281 million [m^3] for injection rate of 3 E 5[Sm^3/day] and injection time t=100-500 days.

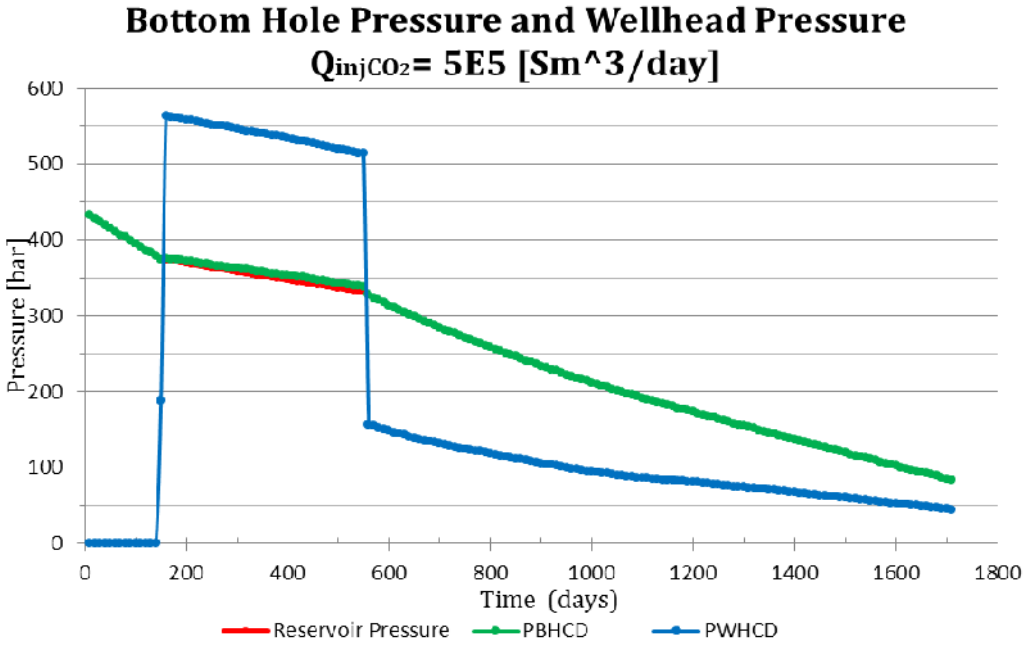

Figure 23 Carbon Dioxide Injection Rate of 5 E5 [Sm3/day] for Unstable Model; Start of Injection= 150 day; Stop of Injection= 550 day Injection Time: 400 day

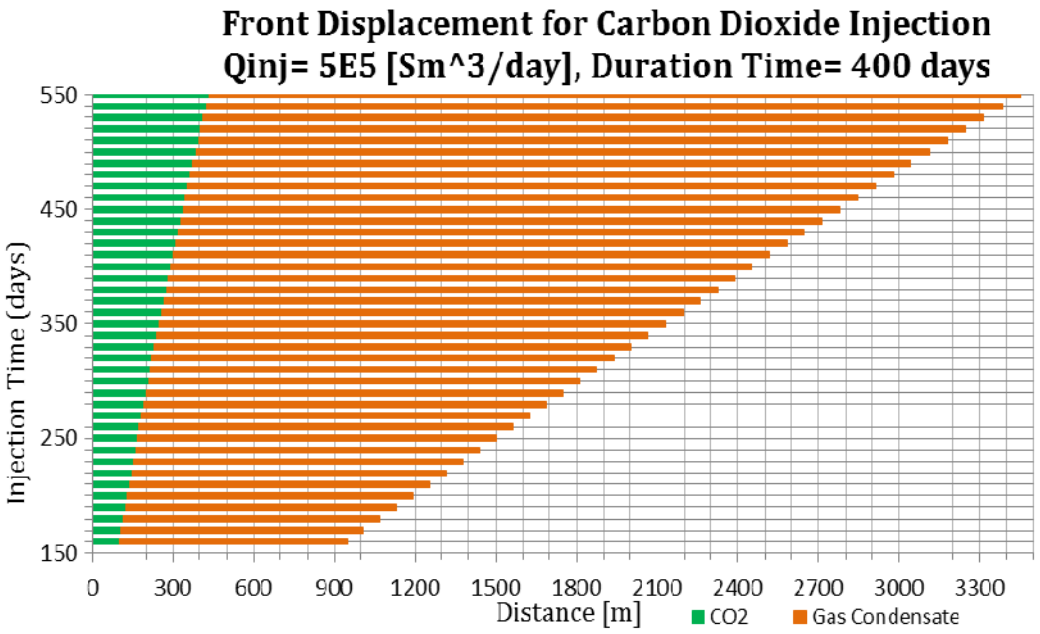

Figure 24 Front Displacement for Carbon Dioxide Injection in Unstable Model; Start of Injection= 150 day; Stop of Injection= 550 day Injection Time: 400 days

One option for duration time of 400 days, it is to start at time t= 150 days, it is not chosen at t=200 day because the main focus is to enlarge to fall into retrograde region, starting at such time does not give a good option. Injection is stopped at t=550 day, breakthrough occurs at time t= 420 day as it is observed in Figure 23 and Figure 24. Carbon dioxide is still a supercritical fluid.

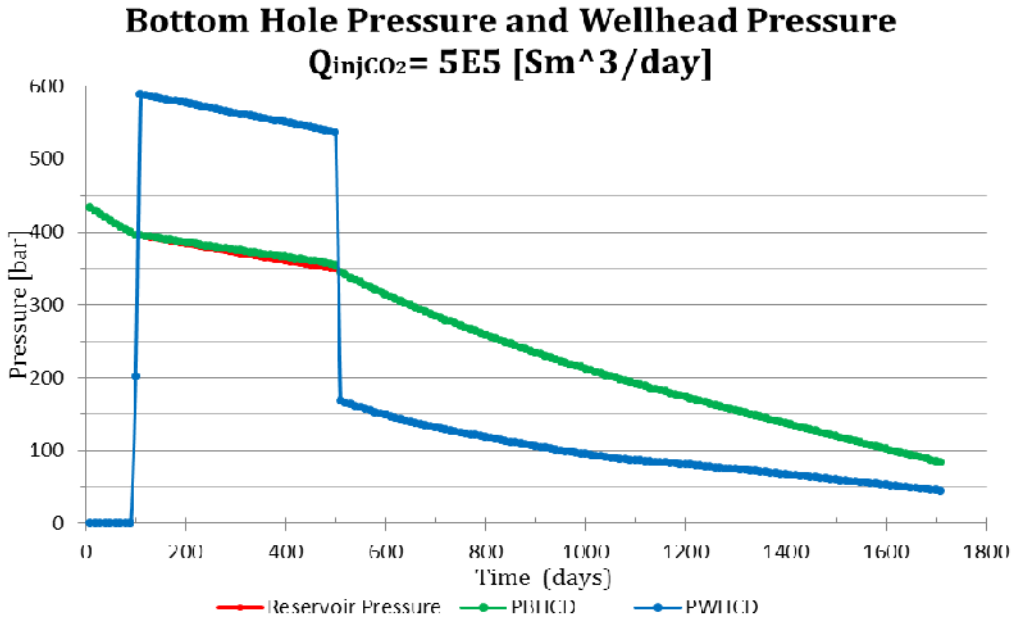

Figure 25 Carbon Dioxide Injection Rate of 5 E5 [Sm3/day] for Unstable Model;
Start of Injection= 100 day; Stop of Injection= 500 day
Injection Time: 400 day

Another option for injection time of 400 days is to start at time t=100 and to stop at time t=500 days. Better performance was observed for this case, injection rate is still 5 E5 [Sm^3/day]. Reservoir pressure was preserved and at the end is 83.5 [bar] and a well head injection pressure P_{wh}= 589 [bar]. Breakthrough at day 440. Substantial increment in total gas production of 0.8546 million [m^3] and total liquid production of 0.3394 million [m^3] compared to the other simulations with different injection time and injection rate.

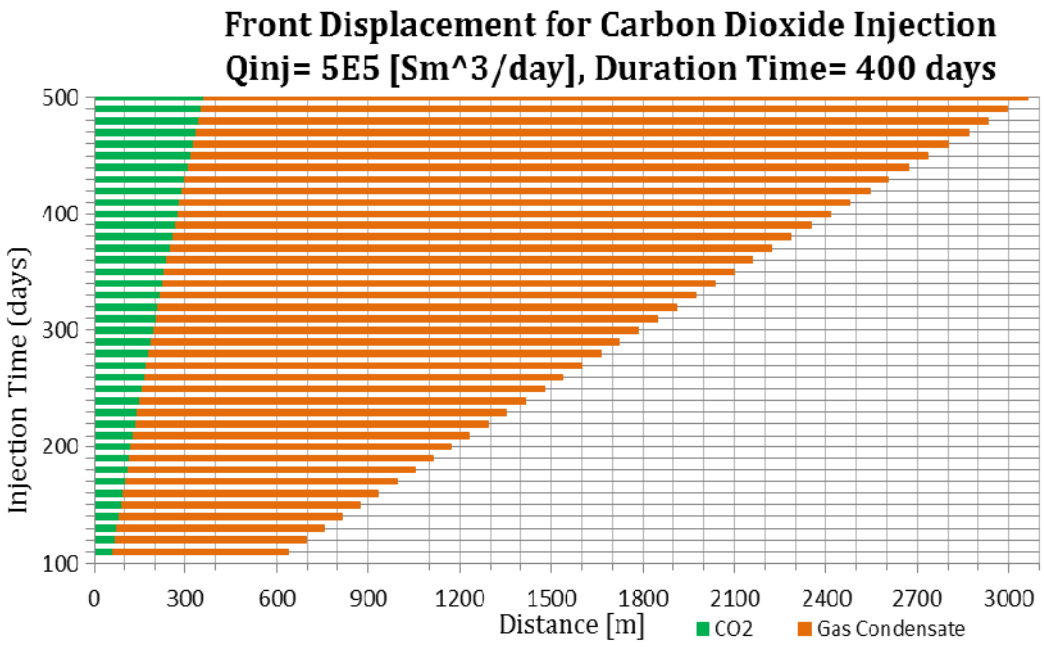

Figure 26 Front Displacement for Carbon Dioxide Injection in Unstable Model; Start of Injection= 100 day; Stop of Injection= 500 day Injection Time: 400 days

4.4.5. Effect of change in Wellhead Temperature for Carbon Dioxide Injection

In Table 12, it is seen results of simulation for different carbon dioxide injection rate q_{injCO2} for a horizontal reservoir (Θ=0) to see effect of temperature in surface conditions to analyze if there is phase change of carbon dioxide when it is traveling downwards to reservoir. It is observed a higher wellhead injection pressure for both injection rates at lower wellhead temperature; the carbon dioxide is in liquid phase if temperature is lower than its critical temperature and in supercritical state when it is above it. Then, there is some possibility for bottom-hole injection pressure to be greater than initial reservoir pressure. There will be some further study of those temperature effects in wellhead injection temperature as it is not advisable to be above initial reservoir pressure.

Injection flow rate [Sm^3/day]	Phase Carbon Dioxide	Wellhead Temperature [K]	Wellhead Pressure at start of injection [bar]
3E5	Liquid	277= 4 C	594.
	Liquid	288= 15 C	591.
	Liquid	293= 20 C	590.
	Supercritical	313 = 40 C	585.
5E5	Liquid	277	597.
	Liquid	288	594.
	Liquid	293	593.
	Supercritical	313	589.

Table 12 Different Wellhead Temperature for Carbon Dioxide Injection of q_{injCO2} of 3E5 and 5E5 [Sm^3/day]

CO_2 SEQUESTRATION IN GAS-CONDENSATE RESERVOIRS

CHAPTER 5

CONCLUSIONS

It can be concluded that injection of carbon dioxide raises reservoir pressure as the important feature for pressure maintenance into the example gas condensate reservoir in this Thesis, it is seen a higher liquid production in comparison to dry gas injection. It was encountered higher values of wellhead injection pressure related directly to flow injection rate when simulating. It is exhibited higher pressure drop in carbon dioxide section for all displacement models and dominates the total flow pressure drop given mainly due to the great differences in density and viscosity between gas condensate (resident gas) and carbon dioxide (injection fluid).

At pressures and temperature typically encountered in the example gas condensate reservoir, CO_2 will behave as a supercritical fluid. Furthermore, it has been analyzed carbon dioxide injection into gas retrograde reservoirs through use of simplified models in several simulations through a linear shaped reservoir.

Verification of physical property calculations for carbon dioxide properties was done comparing results and published data (Reference data). It is found a very good agreement for density and viscosity, main properties for displacement of carbon dioxide into the reservoir.

Mixing in the reservoir due to large density and viscosity of CO_2 relative to gas condensate is limited; this difference is larger at high pressure as carbon dioxide exhibits large changes in density and viscosity with pressure increase especially above its supercritical region.

It has been found limited enhanced gas recovery because of early breakthrough of carbon dioxide into production well. It is believed that is due to effects of permeability. The program assigns equal values of permeability to carbon dioxide and to gas condensate. Therefore, carbon dioxide will move faster through higher permeable zones, this accelerates CO_2 breakthrough.

The particular aspects considered for the effect of impurities in injection stream of CO_2 are the effects which are divided into two categories: physical and chemical. Physical concerns phase behavior, storage capacity, buoyancy. Chemical concerns rock-porosity related to injectivity, well material corrosion. It is studied that the most significant effect is reduction of storage capacity by reduced structural trapping capacity caused by non-condensable impurities; injectivity of impure CO_2 is reduced as a result of lower density; higher buoyancy of impure CO_2 streams reduces the CO_2 trapping in rock pores reducing security of CO_2 storage underground, it is needed deeper depths of injection to alleviate it.

Moreover, combining this technical expertise and fundamentals of carbon dioxide injection, this can contribute to preserve environment while capturing CO_2 emissions and at the same time can increase recovery from such gas condensate reservoirs.

SUGGESTIONS

- When injecting carbon dioxide, there will be some additional costs associated with injection of a corrosive gas.

- Further study taking into account impurities in stream of carbon dioxide to see effects that are assumed to happen in the present Thesis.

- Implementation in the in-house simulator an extension to take into account differences in permeability for CO_2 and gas condensate to enhance simulation, relative permeability as it is discussed in Chapter 2.

REFERENCES

1. Bahadori, A., H.B. Vuthaluru, and S. Mokhatab, *New correlations predict aqueous solubility and density of carbon dioxide.* International Journal of Greenhouse Gas Control, 2009. **3**(4): p. 474-480.

2. Ouyang, L.-B., *New Correlations for Predicting the Density and Viscosity of Supercritical Carbon Dioxide Under Conditions Expected in Carbon Capture and Sequestration Operations.* Open Petroleum Engineering Journal, 2011. **4**: p. 9.

3. Ahmed, T.H., *Hydrocarbon Phase Behavior*. 1989, Gulf Publishing Company: Austin TX, USA.

4. Jarrell, P.M., *Practical Aspects of CO2 Flooding*. Vol. 22. 2002: Richardson, Tex.: Henry L. Doherty Memorial Fund of AIME, Society of Petroleum Engineers.

5. *Available from: http://webbook.nist.gov/chemistry/*.

6. Zabaloy, M.S., V.R. Vasquez, and E.A. Macedo, *Viscosity of pure supercritical fluids.* The Journal of supercritical fluids, 2005. **36**(2): p. 106-117.

7. Vesovic, V., et al., *The Transport Properties of Carbon Dioxide.* Journal of Physical and Chemical Reference Data, 1990. **19**(3): p. 763-808.

8. Fenghour, A., W.A. Wakeham, and V. Vesovic, *The Viscosity of Carbon Dioxide.* Journal of Physical and Chemical Reference Data, 1998. **27**(1): p. 31-44.

9. Stephan, K. and K. Lucas, *Viscosity of Dense Fluids*. 1979: Springer.

10. Heidaryan, E., et al., *Viscosity of pure carbon dioxide at supercritical region: Measurement and correlation approach.* The Journal of Supercritical Fluids, 2011. **56**(2): p. 144-151.

11. Wang J., R.D., Anthony E., Wingston A., *Effects of Impurities on Geological Storage of Carbon Dioxide.* IEA Greenhouse Gas R& D Programme, 2011.

NOMENCLATURE

P_i= Initial Reservoir Pressure [bar]

P_{wh}= Wellhead injection pressure [bar]

T_i= Initial Reservoir Temperature [K]

h= Reservoir thickness [m]

H= Length of well [m]

W= Reservoir width [m]

r_e= Drainage radius [m]

r_w= Wellbore radius [m]

C_A= Dietz shape factor

Ø= Porosity [%]

k= Absolute permeability [mD]

μ= Viscosity [bar-d]

ϱ= Density [kg/m^3]

S_w= Initial water saturation [%]

S= Skin factor

c_w= Water compressibility [bar^{-1}]

c_R= Reservoir compressibility [bar^{-1}]

T_{WH}= Wellhead temperature [K]

ID= Inner Diameter of tubing [m]

ε= Roughness

α= Deviation angle [^{o}]

q_{injCO2}= carbon dioxide injection rate at standard conditions [Sm^3/day]

$q_{critCO2}$= critical carbon dioxide injection rate [m^3/day]

q_{max}= maximum carbon dioxide injection rate [m^3/day]

APPENDIX 1

GRAVITY SEGREGATION DISPLACEMENT

Assumptions:

- Carbon dioxide underrunning resident gas because of higher density of carbon dioxide (injection fluid).
- Gas condensate is drifting upwards due to the great difference in density values between CO_2 (injection fluid) and gas condensate (resident gas).
- Gas condensate will flow over carbon dioxide.
- Up-dip Reservoir.

From Darcy´s Law:

$$u = -\frac{k}{\mu}\rho\frac{\partial}{\partial x}(\Phi)$$

$$q = -\frac{kA}{\mu}\rho\frac{\partial}{\partial x}(\Phi)$$

$$\Phi = phi - potential \qquad \Phi = \frac{P}{\rho} + gz$$

$$q = -\frac{k}{\mu}A\left(\frac{\partial P}{\partial x} + \rho g\frac{\partial z}{\partial x}\right)$$

$$\vec{g} = \left(g_x, g_y\right)$$

$$\vec{g} = \left(g\sin\theta, g\cos\theta\right)$$

For flow of gas condensate and carbon dioxide:

$$\mathrm{q}_{\mathrm{cond}} = -\frac{\mathrm{k}_{\mathrm{cond}}}{\mu_{cond}}A\left(\frac{\partial P_{cond}}{\partial x} - \rho_{cond}\,g_x\right)$$

$$\mathrm{q}_{\mathrm{CO2}} = -\frac{\mathrm{k}_{\mathrm{CO2}}}{\mu_{CO2}}A\left(\frac{\partial P_{CO2}}{\partial x} - \rho_{CO2}\,g_x\right)$$

As carbon dioxide is flowing downwards and gas condensate is flowing upwards:

$$\mathrm{q}_{\mathrm{cond}} = -q_{CO2} \qquad \text{Equation 41}$$

There is no capillary pressure between phases:

$$\frac{\partial P_{cond}}{\partial x} - \frac{\partial P_{CO2}}{\partial x} = 0 \qquad \Rightarrow \frac{\partial P_{cond}}{\partial x} = \frac{\partial P_{CO2}}{\partial x} \qquad \text{Equation 42}$$

Then:

$$\frac{\partial P_{cond}}{\partial x} = -\frac{q_{cond}}{\frac{k_{cond}}{\mu_{cond}} A} + \rho_{cond} g_x$$

$$\frac{\partial P_{CO2}}{\partial x} = -\frac{q_{CO2}}{\frac{k_{CO2}}{\mu_{CO2}} A} + \rho_{CO2} g_x$$

$$\frac{q_{CO2}}{\frac{k_{CO2}}{\mu_{CO2}} A} - \frac{q_{cond}}{\frac{k_{cond}}{\mu_{cond}} A} = \rho_{CO2} g_x - \rho_{cond} g_x$$

From Equation 41:

$$\frac{q_{CO2}}{\frac{k_{CO2}}{\mu_{CO2}} A} + \frac{q_{CO2}}{\frac{k_{cond}}{\mu_{cond}} A} = \left(\rho_{CO2} - \rho_{cond}\right) g_x$$

In terms of mobility $\lambda = \frac{k}{\mu}$ and considering that $A_{CO2} = Wh_{CO2}$ and $A_{cond} = Wh_{cond}$:

$$\frac{q_{CO2}}{\lambda_{CO2} A_{CO2}} + \frac{q_{CO2}}{\lambda_{cond} A_{cond}} = \Delta\rho g_x$$

$$q_{CO2} = \frac{\Delta\rho g_x}{\frac{1}{\lambda_{CO2} A_{CO2}} + \frac{1}{\lambda_{cond} A_{cond}}} \qquad \text{Equation 43}$$

It can also be expressed in terms of mobility ratio end point:

$$M = \frac{\lambda_{displacing\ .\ fluid}}{\lambda_{displaced\ .\ fluid}}$$

For Carbon Dioxide Injection: $M = \frac{\lambda_{CO2}}{\lambda_{cond}} = \frac{\frac{k_{CO2}}{\mu_{CO2}}}{\frac{k_{cond}}{\mu_{cond}}}$

$$q_{CO2} = \frac{\Delta\rho g_x}{\frac{1}{\lambda_{CO2}}\left(\frac{1}{A_{CO2}} + \frac{M}{A_{cond}}\right)}$$

$$q_{CO2} = \frac{\lambda_{CO2}\Delta\rho g_x A_{CO2}}{\left(1 + M\frac{h_{CO2}}{h_{cond}}\right)}$$

Considering $h = h_{CO2} + h_{cond}$

$$q_{CO2} = \frac{k_{CO2}}{\mu_{CO2}} \frac{\Delta\rho g_x W\left(h - h_{CO2}\right)h_{CO2}}{\left[h + (M-1)h_{CO2}\right]}$$

The previous equation can be in terms of h_{CO2} and derived to find minimum value of carbon dioxide flow rate:

$$q_{CO2} = \frac{B\left(h - h_{CO2}\right)h_{CO2}}{\left(h + (M-1)h_{CO2}\right)}$$ Equation 44

$$\frac{d}{d}\left(\frac{q_{CO2}}{h_{CO2}}\right) = 0$$

From derivate formulae:

$$y = \frac{u(x)}{v(x)}$$

$$y = \frac{u'v - uv'}{v^2} \qquad \Rightarrow \frac{dy}{dx} = \frac{vdu - udv}{v^2}$$

$$\frac{d}{d}\left(\frac{q_{CO2}}{h_{CO2}}\right) = \frac{\left[h + (M-1)h_{CO2}\right](h - 2h_{CO2}) - \left[(h - h_{CO2})h_{CO2}\right](M-1)}{\left[h + (M-1)h_{CO2}\right]^2}$$

The numerator can be approximated to $x^2 - 2xy + y^2 = 0$

$$h^2 - 2hh_{CO2} - (M-1)h_{CO2}{}^2 = 0$$

$$h^2 - 2hh_{CO2} + h_{CO2}{}^2 = (M-1)h_{CO2}{}^2 + h_{CO2}{}^2$$

The aim is to find height of carbon dioxide:

$$\left(h - h_{CO2}\right)^2 = Mh_{CO2}{}^2$$

$$h_{CO2} = \frac{h}{\sqrt{M}+1} \qquad \text{Equation 45}$$

Into Equation 44:

$$q_{CO2} = \frac{B(h - h_{CO2})}{\frac{h}{h_{CO2}} + (M-1)}$$

From Equation 45:

$$q_{CO2} = \frac{B\left(h - \frac{h}{\sqrt{M}+1}\right)}{M + \sqrt{M}} \qquad \text{Equation 46}$$

Then the product of $\left(M + \sqrt{M}\right)\left(\sqrt{M}+1\right) = \sqrt{M}\left(1 + 2\sqrt{M} + M\right)$

It can be approximated to a quadratic equation of the form:

$$\left(1+\sqrt{M}\right)^2 = 1^2 + 2\sqrt{M} + M$$

Finally, this into Equation 6 to get maximum flow rate of carbon dioxide for the displacement according to Gravity Segregation Model:

$$q_{CO2} = \frac{Bh\sqrt{M}}{\sqrt{M}\left(1 + 2\sqrt{M} + M\right)}$$

$$q_{CO2} = \frac{k_{CO2}}{\mu_{CO2}} \frac{\Delta\rho g_x Wh}{\left(1+\sqrt{M}\right)^2}$$

$$q_{\max.CO2} = \frac{k_{CO2}}{\mu_{CO2}}\left(\rho_{CO2} - \rho_{cond}\right) g \sin\theta \frac{Wh}{\left(1+\sqrt{M}\right)^2}$$

Pressure Drop Derivation for Gravity Segregation

Darcy´s Law:

$$u = -\frac{k}{\mu}\rho\frac{\partial}{\partial x}(\Phi)$$

$$q = -\frac{kA}{\mu}\rho\frac{\partial}{\partial x}(\Phi)$$

$$q = -\frac{k}{\mu}A\left(\frac{\partial P}{\partial x} + \rho g\frac{\partial z}{\partial x}\right)$$

For linear flow the pressure drop can be expressed in terms of the pressure difference ΔP and a finite length L:

$$\Delta P = -\left(\frac{q\mu}{kWh} \pm \rho g\sin\theta\right)L$$

Pressure drop for Gas condensate and Carbon Dioxide:

$$\Delta P_{cond} = -\left(\frac{q\mu_{cond}}{kWh_{cond}} + \rho_{cond} g\sin\theta\right)L$$

h_{cond} can be found from Equation 45:

$$h = h_{CO2} + h_{cond}$$

$$h_{cond} = \frac{h\sqrt{M}}{\sqrt{M}+1}$$ Equation 47

$$\Delta P_{CO2} = -\left(\frac{q\mu_{CO2}}{kWh_{CO2}} - \rho_{CO2} g\sin\theta\right)L$$

Finally, total pressure drop:

$$\Delta P_{total} = \Delta P_{cond} + \Delta P_{CO2}$$

$$\Delta P_{total} = -\left[\frac{q}{KW}\left(\frac{\mu_{cond}}{h_{cond}} + \frac{\mu_{CO2}}{h_{CO2}}\right) - \left(\rho_{CO2} - \rho_{cond}\right)g\sin\theta\right]L$$

APPENDIX 2

STABLE DISPLACEMENT

Assumptions:

- Down-dip Reservoir.
- Carbon dioxide underrunning resident gas.
- Mixing or Diffusion is neglected due to great difference in densities between fluids.
- There is change in phase for carbon dioxide if low pressure is achieved.
- Relative permeability end point is applied for $k_{CO2} = kk'_{r.CO2}$ and $k_{cond} = kk'_{r.cond}$

Applying Darcy´s Law for linear flow, the one dimensional equation for flow of gas condensate (resident gas) and carbon dioxide (injection fluid):

$$q_{cond} = -\frac{k_{cond}}{\mu_{cond}} A\rho_{cond} \frac{\partial}{\partial x}\left(\Phi_{cond}\right) = -\frac{kk'_{r.cond}}{\mu_{cond}} A\left(\frac{\partial P_{cond}}{\partial x} + \frac{\rho_{cond} g \sin\theta}{1.0133E6}\right)$$

$$q_{CO2} = -\frac{k_{CO2}}{\mu_{CO2}} A\rho_{CO2} \frac{\partial}{\partial x}\left(\Phi_{CO2}\right) = -\frac{kk'_{r.CO2}}{\mu_{CO2}} A\left(\frac{\partial P_{CO2}}{\partial x} + \frac{\rho_{CO2} g \sin\theta}{1.0133E6}\right)$$

In terms of velocity $q = uA$ and if displacement of incompressible displacement is stable then at all points on the interface, gas condensate and carbon dioxide will have the same velocity.

$$-u_T \frac{\mu_{cond}}{k_{cond}} - \frac{\rho_{cond} g \sin\theta}{1.0133E6} = \frac{\partial P_{cond}}{\partial x}$$

$$-u_T \frac{\mu_{CO2}}{k_{CO2}} - \frac{\rho_{CO2} g \sin\theta}{1.0133E6} = \frac{\partial P_{CO2}}{\partial x}$$

The direction of flow is normal to x direction with respect to the imaginary horizontal plane.

$$\frac{\partial P_{cond}}{\partial x} - \frac{\partial P_{CO2}}{\partial x} = u_T\left(\frac{\mu_{CO2}}{k_{CO2}} - \frac{\mu_{cond}}{k_{cond}}\right) + \frac{\left(\rho_{CO2} - \rho_{cond}\right) g \sin\theta}{1.0133E6}$$

$$\frac{\partial P_C}{\partial x} = \frac{\partial P_{cond}}{\partial x} - \frac{\partial P_{CO2}}{\partial x}$$

$$\frac{\partial P_C}{\partial x} = u_T\left(\frac{\mu_{CO2}}{k_{CO2}} - \frac{\mu_{cond}}{k_{cond}}\right) + \frac{\Delta\rho g \sin\theta}{1.0133E6} \qquad \text{Equation 48}$$

For capillary pressure:

$$\frac{\partial P_C}{\partial x} = -\frac{\Delta\rho g \cos\theta}{1.0133E6}\frac{dy}{dx}$$

Then into Equation 48:

$$u_T\left(\frac{\mu_{cond}}{k_{cond}} - \frac{\mu_{CO2}}{k_{CO2}}\right) = \frac{\Delta\rho g \sin\theta}{1.0133E6} + \frac{\Delta\rho g \cos\theta}{1.0133E6}\frac{dy}{dx}$$

In terms of total flow rate $q_T = u_T A$ and mobility ratio end point M:

$$\frac{q_T}{A}\left(\frac{1}{\frac{kk'_{r.cond}}{\mu_{cond}}} - \frac{1}{\frac{kk'_{r.CO2}}{\mu_{CO2}}}\right) = \frac{\Delta\rho g}{1.0133E6}\left(\sin\theta + \cos\theta\frac{dy}{dx}\right)$$

$$M = \frac{\lambda_{CO2}}{\lambda_{cond}} = \frac{\frac{kk'_{r.CO2}}{\mu_{CO2}}}{\frac{kk'_{r.cond}}{\mu_{cond}}}$$

$$(M-1) = \frac{kk'_{r.CO2}}{\mu_{CO2}}\frac{A}{q_T}\frac{\Delta\rho g \sin\theta}{1.0133E6}\left(1 + \frac{1}{\tan\theta}\frac{dy}{dx}\right) \qquad \text{Equation 49}$$

It is stated a Gravity Number GN which contains all the parameters:

$$GN = \frac{kk'_{r.CO2}}{\mu_{CO2}}\frac{A}{q_T}\Delta\rho g \sin\theta$$

To solve the slope of interface for stable flow,

$$\frac{dy}{dx} = \left(\frac{M-1-GN}{GN}\right)\tan\theta$$

It is known:

$$\frac{dy}{dx} = -\tan\beta \Rightarrow \tan\beta = \left(\frac{GN-M+1}{GN}\right)\tan\theta$$

When Gravity Number is GN= M – 1, the carbon dioxide will underrun resident gas in the form of a tongue, solving for this condition in Darcy units [resbbl/day]:

$$q_T = 4.9E-4\frac{kk'_{r.CO2}}{\mu_{CO2}}\frac{A\Delta\rho g\sin\theta}{(M-1)}$$

This is the so called carbon dioxide "critical rate" for bypassing which in [m^3/day]:

$$q_{critCO2} = 8.64E-8\frac{k_{CO2}}{\mu_{CO2}}A\frac{\Delta\rho g\sin\theta}{(M-1)}$$

Pressure Drop Derivation for Stable Displacement

From Darcy´s Law in differential form:

$$q = -\frac{kA}{\mu}\frac{dP}{dx}$$

Expressed in terms of ϕ phi-potential:

$$q = -\frac{kA}{\mu}\rho\frac{\partial}{\partial x}(\Phi)$$

$$\mathrm{q} = -\frac{\mathrm{k}}{\mu}A\left(\frac{\partial P}{\partial x}+\rho g\frac{\partial z}{\partial x}\right)$$

Then solving to know the pressure change,

$$\mathrm{q} = -\frac{\mathrm{k}}{\mu}A\left(\frac{\Delta P}{\Delta x}\pm\rho g\sin\theta\right)$$

$$\Delta\mathrm{P} = -\left(\frac{q\mu}{kA}\pm\rho g\sin\theta\right)\Delta x$$

For gas condensate and carbon dioxide:

$$\Delta\mathrm{P}_{\mathrm{cond}} = -\left(\frac{q_{cond}\,\mu_{cond}}{kA}-\rho_{cond}\,g\sin\theta\right)\Delta x_{cond}$$

$$\Delta\mathrm{P}_{\mathrm{CO2}} = -\left(\frac{q_{CO2}\,\mu_{CO2}}{kA}-\rho_{CO2}\,g\sin\theta\right)\left(L-\Delta x_{cond}\right)$$

The minus sign in the phi-potential indicates that the potential for a down dip is minor than for an up dip reservoir.

Applying Law of Mass Conservation:

$$m_{CO2} = m_{cond}$$

$$q_{cond} = \frac{\rho_{CO2}}{\rho_{cond}} q_{CO2}$$

Because of the flow direction for stable displacement, total pressure drop is for series flow:

$$\Delta P_{flow} = \Delta P_{cond} + \Delta P_{CO2}$$

$$\Delta P_{total} = -\left[\left(\frac{q_{cond}\mu_{cond}}{kA}\Delta x_{cond} + \frac{q_{CO2}\mu_{CO2}}{kA}\left(L - \Delta x_{cond}\right)\right) + \left(\Delta\rho\Delta x_{cond} - \rho_{CO2} L\right) g\sin\theta\right]$$

Where $\Delta\rho = \left(\rho_{CO2} - \rho_{cond}\right)$ and the term $\left(\Delta\rho\Delta x_{cond} - \rho_{CO2} L\right) g\sin\theta$ account for the gravity term of the equation.

APPENDIX 3

UNSTABLE DISPLACEMENT

Assumptions:

- Carbon Dioxide (injection fluid) is less viscous than gas condensate (resident gas).
- The more viscous resident gas is displaced by carbon dioxide in which displacement front is not stable.
- Gravitational effects and rock compressibility are negligible.
- Microscopic mixing between fluids is neglected.

Darcy´s Law in x direction where flow takes place:

$$u = -\lambda \nabla \Phi$$

$$u = -\lambda \nabla \left(P + \vec{g} \rho \vec{z} \right)$$

$$u = -\lambda \left(\nabla P + \rho \nabla g z \right)$$

$$u = -\lambda \left(\nabla P + \rho \vec{g} \right)$$

Then the flow velocities for gas condensate and carbon dioxide:

$$u_{\text{cond}} = -\lambda_{cond} \nabla \Phi_{cond} \qquad \text{Equation 50}$$

$$u_{\text{CO2}} = -\lambda_{CO2} \nabla \Phi_{CO2} \qquad \text{Equation 51}$$

$$u_{\text{cond}} = -\lambda_{cond} \left(\frac{\partial P_{cond}}{\partial x} + \rho_{cond} g_x \right)$$

$$u_{\text{CO2}} = -\lambda_{CO2} \left(\frac{\partial P_{CO2}}{\partial x} + \rho_{CO2} g_x \right)$$

Flow potential is continuous across flow:

$$\nabla \Phi_{\text{cond}} = \nabla \Phi_{CO2}$$

$$\frac{\partial \text{P}_{\text{cond}}}{\partial \text{x}} - \frac{\partial P_{CO2}}{\partial x} = \rho_{CO2} g_x - \rho_{cond} g_x$$

Capillary Pressure:

$$\frac{\partial}{\partial x}\left(P_{cond} - P_{CO2}\right) = \left(\rho_{CO2} - \rho_{cond}\right)g_x \quad \Rightarrow \frac{\partial P_C}{\partial x} = \Delta\rho g_x$$ Equation 52

For the end point mobility ratio M $M = \frac{\lambda_{CO2}}{\lambda_{cond}}$ and Equation 50 and 51:

$$\frac{u_{CO2}}{u_{cond}} = \frac{-\lambda_{CO2}\nabla\Phi_{CO2}}{-\lambda_{cond}\nabla\Phi_{cond}} = \frac{\lambda_{CO2}}{\lambda_{cond}} \Rightarrow \frac{u_{CO2}}{u_{cond}} = M$$ Equation 53

Incompressible displacement occurs if:

$$q_{total} = q_{cond} + q_{CO2} = q_{inj}$$ Equation 54

In terms of phase velocities for carbon dioxide (injection fluid) and gas condensate (resident gas):

$$q_{cond} = u_{cond} A_{cond} = u_{cond}\left(Wh_{cond}\right)$$ Equation 55

$$q_{CO2} = u_{CO2} A_{CO2} = u_{CO2}\left(Wh_{CO2}\right)$$ Equation 56

From Equation 53 and 55 into Equation 54:

$$q_{CO2} = q_{total} - u_{cond}\left(Wh_{cond}\right)$$

$$= q_{total} - \frac{u_{CO2}}{M}\left(Wh_{cond}\right)$$

Moreover, Equation 56 into previous equation:

$$q_{CO2} = q_{total} - \frac{q_{CO2}}{\left(Wh_{CO2}\right)}\frac{1}{M}\left(Wh_{cond}\right)$$

In the aim to find carbon dioxide flow rate:

$$q_{CO2} = \frac{q_{total} Mh_{CO2}}{(M-1)h_{CO2} + h}$$ Equation 57

Applying material balance, S being saturation of carbon dioxide that travels through reservoir:

$$\Delta q_{CO2} = \Delta A \frac{\Delta x}{\Delta t}$$

$$\frac{\Delta q_{CO2}}{\Delta x} = \frac{\Delta\left(Wh_{CO2}\phi\Delta S\right)}{\Delta t}$$

In differential form and with height of carbon dioxide varying when displacement takes place:

$$\frac{d}{dx}\left(q_{CO2}\right)=\frac{d}{dt}\left(h_{CO2}\phi W\Delta S\right)$$

$$\frac{d}{dx}\left(q_{CO2}\right)=\frac{d}{dx}\left(h_{CO2}\right)\frac{dx}{dt}\left(\phi W\Delta S\right)$$

Fluids flowing with velocity in x direction of flow, it follows:

$$v_x=v(h)=\frac{dx}{dt}$$

$$\frac{dx}{dt}=\frac{d}{dx}\left(q_{CO2}\right)\frac{dx}{dh_{CO2}}\frac{1}{\phi W\Delta S}$$

$$\frac{dx}{dt}=\frac{1}{\phi W\Delta S}\frac{\partial}{\partial h_{CO2}}\left(q_{CO2}\right)$$

From Equation 57 q_{CO2} into previous equation of velocity:

$$\frac{dx}{dt}=\frac{1}{W\phi\Delta S}\frac{\partial}{\partial h_{CO2}}\left(\frac{q_{total}Mh_{CO2}}{(M-1)h_{CO2}+h}\right)$$

From derivate formulae:

$$y=\frac{u(x)}{v(x)}$$

$$y'=\frac{u'v-uv'}{v^2}\Leftrightarrow\frac{dy}{dx}=\frac{vdu-udv}{v^2}$$

$$\frac{\partial}{\partial h_{CO2}}\left(\frac{q_{total}Mh_{CO2}}{(M-1)h_{CO2}+h}\right)=\frac{q_{total}M\left[(M-1)h_{CO2}+h\right]-\left(q_{total}Mh_{CO2}\right)(M-1)}{\left[(M-1)h_{CO2}+h\right]^2}$$

Finally velocity in direction x that can be applied to find the position of front and rear displacement respectively:

$$v_x = \frac{1}{\phi W \Delta S} \frac{q_{total} Mh}{\left[h + (M-1)h_{CO2}\right]^2} \qquad \Leftrightarrow v(h) = \frac{1}{\phi W \Delta S} \frac{q_{total} Mh}{\left[h + (M-1)h_{CO2}\right]^2}$$

At end of front displacement of carbon dioxide injection, $h_{CO2} \rightarrow 0$

$$x_f = \frac{q_{total} t}{\phi W h} M$$

At rear of front displacement, $h_{CO2} \rightarrow h$

$$x_r = \frac{q_{total} t}{\phi W h} \frac{1}{M}$$

x_f and x_r are the front and rear of viscous fingering zone respectively. Next, length of viscous fingering zone can be calculated:

$$L_{VF} = x_f - x_r = \frac{q_{total} t}{\phi W h}\left(M - \frac{1}{M}\right)$$

Pressure Drop Derivation for Unstable Displacement

A. Pressure drop in viscous fingering zone

First, volumetric flux of carbon dioxide and gas condensate:

$$q_{CO2} = -\frac{k_{CO2}}{\mu_{CO2}} WhS\left(\frac{dP}{dx}\right) = -\lambda_{CO2} WhS\left(\frac{dP}{dx}\right)$$

$$q_{cond} = -\frac{k_{cond}}{\mu_{cond}} Wh(1-S)\left(\frac{dP}{dx}\right) = -\lambda_{cond} Wh(1-S)\left(\frac{dP}{dx}\right)$$

Second, total volumetric flux:

$$q_{total} = q_{CO2} + q_{cond}$$

$$q_{total} = -Wh\left(\frac{dP}{dx}\right)\left[\lambda_{CO2} S + \lambda_{cond}(1-S)\right]$$

Introducing end point mobility ratio M concept then:

$$dP = -\frac{q_{total}\,\mu_{cond}}{Whk_{cond}}\left[\frac{1}{1+(M-1)S}\right]dx \qquad \text{Equation 58}$$

Saturation profile as a function of time gives:

$$x_S = \frac{q_{total}}{\phi Wh}t\left\{\frac{M}{\left[1+(M-1)S\right]^2}\right\} \qquad \text{Equation 59}$$

Solving to find saturation is:

$$S = \frac{\sqrt{\frac{q_{total}\,tM}{\phi Whx_S}}-1}{M-1} \qquad \text{Equation 60}$$

Introducing Equation 60 and Integrating Equation 58:

$$\int_{P0}^{P1} dP = -\frac{q_{total}\,\mu_{cond}}{Whk_{cond}}\sqrt{\frac{\phi Wh}{q_{total}\,tM}}\int_0^{Lvf}\sqrt{x_S}\,dx$$

$$\Delta P = -\frac{2}{3}\frac{q_{total}\,\mu_{cond}}{Whk_{cond}}\sqrt{\frac{\phi Wh}{q_{total}\,tM}}\left[x_S^{3/2}\right]_0^{Lv}$$

Next, Equation 59 for saturation profile into previous equation, finally:

$$\Delta P_{VF} = -\frac{2}{3}\frac{q_{total}^{\,2}t}{\phi(Wh)^2}\frac{\mu_{cond}}{k_{cond}}\frac{(M^2-1)^{3/2}}{M^2}$$

Total Pressure Drop for series flow:

$$\Delta P_{TOTAL} = \Delta P_{CO2} + \Delta P_{VF} + \Delta P_{cond}$$

B. Pressure drop in Carbon Dioxide and Gas Condensate zone

From Darcy´s Law:

$$q = -\frac{k}{\mu}A\frac{\Delta P}{\Delta x}$$

$$L = \Delta x_{CO2} + L_{VF} + \Delta x_{cond}$$

$$\Delta P_{CO2} = -\frac{q_{CO2}}{A}\frac{\mu_{CO2}}{k_{CO2}}\Delta x_{CO2}$$

$$\Delta P_{cond} = -\frac{q_{cond}}{A}\frac{\mu_{cond}}{k_{cond}}\left(L - \Delta x_{CO2} - L_{VF}\right)$$

$$\Delta P_{TOTAL} = -\frac{1}{Wh}\left[\frac{q_{CO2}}{\lambda_{CO2}}\Delta x_{CO2} + \frac{q_{cond}}{\lambda_{cond}}\left(L - \Delta x_{CO2} - L_{VF}\right) - \frac{2}{3}\frac{q_{total}{}^{2}t}{\phi Wh\lambda_{cond}}\frac{\left(M^{2}-1\right)^{3/2}}{M^{2}}\right]$$

However, when a more viscous fluid displaces a less viscous fluid does not create viscous fingering, this is reflected when mobility viscosity ratio M is less than 1 i.e., gas condensate being less viscous and carbon dioxide being more viscous. Due to great change in behavior of carbon dioxide with pressure and temperature, at higher pressures than its critical pressure and critical temperature, the values of its viscosity are of a dense gas and higher than of resident gas. Nevertheless, while reservoir is being depleted, reservoir pressure will be lowering and a phase change exists if those values of reservoir temperature and pressure are lower than its critical values. Then, a change in the mobility ratio M being higher than 1, in this case, a displacement of a less viscous fluid (carbon dioxide) to a more viscous fluid (gas condensate) takes place; carbon dioxide starts fingering. Next, all the equations described liens above characterize the displacement: “unstable displacement”.

APPENDIX 4

INPUT DATA FOR SIMULATION

```
*   **** Start data file NGASDATA.DAT
*
*   Data file name (max. 70 characters); text
*    12345678901234567890123456789012345678901234567890123456789012345678901234567890
    'Project: Natural Gas Reservoir Simulation: Material balance.'
    'Part: Natural Depletion; Extension of program with multi well option'
    'Extension with gas (re)injection (material balance)'
    'Extension with simulation of displacement mechanisms in (re)injection process'
*
*   *** Program Data
*
*   DCHCK=1 Data check mode; No material balance is done.
*   DCHCK=0 Full simulation. [integer]
*   MAXSTEP Number of simulation steps; Program is terminated at simulation step NSTEP [integer]
*   NPRINT   Number of sequent plotting parameter; Printing to file is done for every
*             NPRINT simulation step. [integer]
*   SP=1,100 Short LOG printout; Full printout and printing of every 1 to 100 time step
*            SP=1 gives a short hand presentation of every timestep. [integer]
*
*       DCHCK MAXSTEP NPRINT SP
        0          4000       1          1
*
*   *** Simulation Data:
*
*   PERR       Error limit in pressure calculations. [real]
*   GPGERR     Error limit in volume calculations. [real]
*   DP         Pressure step in pseudo pressure calculation. [real]
*   PREF       Pressure reference in pseudo pressure calculation. [real]
*   CAERR      Error limit in calculation of Dietz-factor. [real]
*
*       PERR   GPGERR   DP  PREF   CAERR
        0.5    1D-07    10.  10.    0.01
*
*   *** Volume and Block Data
*
*   BNAME      Name of individual block, maximum 5 characters. [String]
*   VPORINIT Pore volume of block {=PI*(RADE-RADW)**2*THICK*PORO} (Rm3 ) [real].
*   RADE       Characteristic radius of block (m). [real]
*   RADW       Well bore radius (m). [real]
*   THICK      Netto vertical thickness of block (m). [real]
*
*       BNAME     VPORINIT   RADE  RADW  THICK
        'BLK01'    4D+6       350.   0.175  50.
*
*   *** Block Characteristics:
*
*   PORO     Porosity of block. [real]
*   SWINIT   Initial water saturation [real]
*   PERM     Absolute permeability in block (mD). [real]
*   CA       Dietz shape factor (CA circle=31.62). [real]
*   DARCY    Non-Darcy factor. (day/m3) [real]
*   SKIN     Skin factor. [real]
```

```
*
*       PORO    SWINIT  PERM    CA      DARCY   SKIN  Block no.
        0.20      0.2     100.    31.62   5.D-06   0.0   1          BLK01
*
*   *** General Reservoir Data
*
*   PRS         Initial reservoir pressure (bar). [real]
*   TEMP        Initial reservoir temperature (Kelvin). [real]
*   PRSSC       Atmospheric pressure (bar). [real]
*   TEMPSC      Normal reference temperature (Kelvin). [real]
*   COMW        Water compressibility (1/bar). [real]
*   COMR        Reservoir compressibility (1/bar). [real]
*
*       PRS     TEMP    PRSSC   TEMPSC   COMW      COMR
        437.0   392.0    1.01     288.0    4.35D-05  4.5D-05
*
*   *** Well Production Data
*
*   NWELLS   Total number of wells in the reservoir. [integer]
*
*       NWELLS
        1
*
*   TSTART   Start up time (in days) for sequent wells. Different wells may start up at the same time (day).
*            Start up time (day) is not allocated to any particular well. [real]
*
*       1  2  3  4  5
        0.
*
*   QMIN      Minimum well rate (Sm3/day). [real]
*   QMAX      Maximum well rate (Sm3/day). [real]
*   QPLAT     Plateau reservoir rate (Sm3/day) [real]
*
*       QMIN       QMAX       QPLAT
        1.0D+05    5.0D+05    5.0D+05
*
*   TBP      Time step length in build up period (days). [real]
*   TPP      Time step length in production period (days). [real]
*   TDP      Time step length in decline period (days). [real]
*
*       TBP    TPP    TDP
        10.    10.    3.
*
*   CALCWHP  Decides whether production should be controlled by minimum bottom hole pressure or by minimum
*            wellhead pressure.[integer]
*       CALCWHP=0, Bottom hole pressure controls production.
*       CALCWHP=1, Wellhead pressures controls production.
*
*       CALCWHP
        1
*
*   BHPM     Minimum bottom-hole pressure (bar). Production is stopped when Minimum Bottom hole Pressure is
*            reached. [real]
*           (Minimum bottom-hole pressure should be within the range of the PVT data)
*   WHPM     Minimum Wellhead Pressure (bar). Production is stopped when Minimum Wellhead Pressure is
*            reached. [real]
```

```
*
*       BHPM   WHPM
        50.    20.
*
*  *** Production Well Tubing Data
*
*  WELLGHT    Length of well (m).[real]
*  TUBDIAM    Inner diameter of tubing (m).[real]
*  TUBR       Absolute roughness of tubing (m).[real]
*  WDEVANG    Deviation angle of wells (degrees).[real]
*  TEMPWH     Wellhead temperature (Kelvin).[real]
*
*       NB!! If Wellhead Temperature is the same as reservoir temperature, it must be given a value slightly below
*       reservoir temperature.
*
*       WELLGHT  TUBDIAM  TUBR    WDEVANG TEMPWH  WELL NO.
        3500.    0.200    1.5D-5  0.0     313.    1
*       3500.    0.100    1.5D-5  0.0     313.    2
*
*       *** Well Injection Data
*
*  INWELLS   Total number of injection wells in the reservoir. [integer]
*            ** For Simulation of Displacement Mechanisms, INWELLS = 1
*
*       INWELLS
        1
*
*  TINSTART Defines the startup time for gas injection (days) [real].
*  TINSTOP    Define the stop time for gas injection (days) [real].
*
*       TINSTART    TINSTOP
        0           0
*
*  TINCDSTART    Defines the startup time for CO2 injection (days) [real].
*  TINCDSTOP     Defines the stop time for CO2 injection (days) [real].
*
*       TINCDSTART    TINCDSTOP
        100           500
*
*  QIN          Defines the injection gas rate (Sm3/day) [real].
*  QINJCD       Defines the Carbon Dioxide Injection rate (Sm3/day) [real].
*
*       QIN           QINJCD
        0             3D+05
*
*  *** Injection Well Tubing Data
*
*  INWELLGHT    Length of well (m).[real]
*  INTUBDIAM    Inner diameter of tubing (m).[real]
*  INTUBR       Absolute roughness of tubing (m).[real]
*  INWDEVANG    Deviation angle of wells (degrees).[real]
*  INTEMPWH     Wellhead temperature (Kelvin).[real]
*
*       NB!! If wellhead temperature is the same as reservoir temperature, it must be given a value slightly below
*       reservoir temperature.
*
```

```
*
*       INWELLGHT  INTUBDIAM  INTUBR  INWDEVANG  INTEMPWH  INWELL NO.
        3500.      0.200      1.5D-5  0.0        313.      1
*
*  *** P drop calculation due to Injection data (NEW)
*
*  LOBS      Observation length of reservoir (m). [real]
*  WIDTH     Reservoir width (m). [real]
*  THETA     Res. angle (degree), (value between -90 to 90)
*
*       LOBS  WIDTH  THETA
        300   100    0
*
*  *** Water data
*
*  WATINF=1 Water influx/production controlled as fraction of production.
*             (Only WPFRAC and WEFRAC are relevant parameters.) [Integer]
*  WATINF=2 Water flux from aquifer is included. [integer]
*
*       WATINF
         1
*
*  WPFRAC   Water production as fraction of gas production. [real]
*  WEFRAC   Water influx as fraction of gas production. [real]
*           (A non-zero WPFRAC has normally to be accompanied by a non-zero WEFRAC.)
*
*       WPFRAC  WEFRAC
         0.0     0.0     BLK01
*
*  WTYPE=1    Radial aquifer. [integer]
*  WTYPE=2    Linear aquifer. [integer]
*  WFINITE=1 Finite aquifer. [integer]
*  WFINITE=2 Infinite aquifer. [integer]
*  WALPHA     Angle of sector within which aquifer water encroaches (degree). [real]
*  WCOMP      Aquifer compressibility coefficient (rock and water) (1/bar). [real]
*  WLENGTH  Aquifer length (linear aquifers) (m). [real]
*  WPERM      Aquifer permeability (mD). [real]
*  WPORO      Aquifer porosity. [real]
*  WRADB      Radius of aquifer inner boundary (m). [real]
*  WRADE      Radius of aquifer outer boundary (m). [real]
*  WTHICK     Aquifer thickness (m). [real]
*  WVISC      Water viscosity (mPa.s). [real]
*  WWIDTH     Aquifer width (m). [real]
*
* WTYPE WFINITE WALPHA WCOMP WLENGTH WPERM  WPORO WRADB  WRADE  WTHICK WVISC
* WWIDTH
   1       2       360.    5.D-5   1535.   1.0     0.2     500.    1000.   50.     1.0
1535.   BLK01
*
*  *** PVT data
*
*  NTAB    Number of PVT-table elements
*
*            NTAB
             28
*
```

```
*  PRS      Pressure [bar]
*  TEMP     Temperature [K]
*  MWT      Mixture mol weight [g/mol]
*  MWTG     Gas mol weight [g/mol]
*  MWTL     Liquid mol weight [g/mol]
*  GASF     Gas mol fraction
*  Z        Gas phase Z-factor
*  Z2       Mixture, two-phase Z-factor
*  ZIN      Gas phase Z-factor; Injection gas
*  ZCD      Z Factor; carbon dioxide
*
*    PRS    TEMP    MWT     MWTG    MWTL    GASF      Z        Z2       ZIN      ZCD      NTAB
      550.   392.   26.56   26.56   26.56   0.9517   1.1142   1.1143   1.2400   0.9184   1
      530.   392.   26.56   26.56   26.56   0.9517   1.1142   1.1143   1.2350   0.9001   2
      510.   392.   26.56   26.56   26.56   0.9517   1.1142   1.1143   1.2110   0.8819   3
      490.   392.   26.56   26.56   26.56   0.9517   1.1142   1.1143   1.1871   0.8629   4
      470.   392.   26.56   26.56   26.56   0.9517   1.1142   1.1143   1.1631   0.8434   5
      445.   392.   26.56   26.56   26.56   0.9517   1.1142   1.1143   1.1142   0.8189   6
      370.   392.   26.56   26.56   26.56   0.95171  1.0258   1.0258   1.0258   0.7456   7
      350.   392.   26.57   26.42   90.14   0.95240  1.0035   1.0045   1.0035   0.7261   8
      320.   392.   26.57   26.19   89.32   0.95349  0.9721   0.9743   0.9721   0.6967   9
      300.   392.   26.59   26.03   88.19   0.95438  0.9530   0.9556   0.9530   0.6771   10
      280.   392.   26.61   25.83   87.18   0.95556  0.9356   0.9385   0.9356   0.6694   11
      260.   392.   26.65   25.61   86.86   0.95705  0.9206   0.9233   0.9206   0.6617   12
      240.   392.   26.72   25.36   87.52   0.95883  0.9082   0.9102   0.9082   0.6539   13
      220.   392.   26.81   25.11   89.16   0.96061  0.8986   0.8994   0.8986   0.6462   14
      200.   392.   26.94   24.88   91.68   0.96259  0.8920   0.8994   0.8920   0.6384   15
      180.   392.   27.13   24.66   95.05   0.96446  0.8886   0.8910   0.8886   0.6674   16
      160.   392.   27.38   24.47   99.27   0.96624  0.8885   0.8851   0.8885   0.6963   17
      140.   392.   27.95   24.30   104.49  0.96783  0.8916   0.8808   0.8916   0.7252   18
      120.   392.   28.52   24.18   110.81  0.96921  0.8979   0.8807   0.8979   0.7541   19
      100.   392.   29.33   24.10   118.48  0.97010  0.9073   0.8837   0.9073   0.7830   20
      80.    392.   30.51   24.08   127.84  0.97050  0.9197   0.8862   0.9197   0.8265   21
      60.    392.   32.36   24.16   139.47  0.97079  0.9348   0.8864   0.9348   0.8701   22
      40.    392.   35.59   24.41   154.40  0.97089  0.9524   0.8778   0.9524   0.9131   23
      30.    392.   37.00   24.50   160.00  0.97090  0.9605   0.8720   0.9605   0.9341   24
      20.    392.   39.00   24.60   170.00  0.97092  0.9700   0.8690   0.9700   0.9551   25
      10.    392.   40.00   24.70   178.00  0.97094  0.9800   0.8630   0.9800   0.9759   26
      1.01   392.   42.00   25.00   185.00  0.97099  0.9900   0.8580   0.9900   0.9943   27
      1.01   288.   42.00   25.00   185.00  0.95171  0.9900   0.8580   0.9900   0.9943   28
*
*  *** Data for Liang Biao Density Correlation
*
*        BO      Zero Density Coefficient [real]
*        B1      One Density Coefficient [real]
*        B2      Two Density Coefficient [real]
*        B3      Three Density Coefficient [real]
*        B4      Four Density Coefficient [real]
*
*        BO                  B1                  B2                  B3                  B4

         -2.1483221D+05      4.7571461D+02       -3.7139002D-01      1.2289074D-04       1.4664080D-08
         1.1681166D+04       -2.6192503D+01      2.0724889D-02       -6.9300638D-06      8.3380087D-10
         -2.3022367D+02      5.2151342D-01       -4.1690828D-04      1.4063172D-07       -1.7042424D-11
         1.9674289           -4.4945111D-03      3.6229757D-06       -1.2309953D-09      1.5008789D-13
```

```
      -6.1848428D-03    1.4230588D-05   -1.1550509D-08    3.9484174D-12   -4.8388266D-16
*
*     B5     Five Density Coefficient [real]
*     B6     Six Density Coefficient [real]
*     B7     Seven Density Coefficient [real]
*     B8     Eight Density Coefficient [real]
*     B9     Nine Density Coefficient [real]
*
*     B5                B6                B7                B8                B9

      6.8973827D+02     2.2136925D-01    -5.1187249D-05     5.5179712D-09    -2.1841529D-13
      2.7304792        -6.5472683D-03     2.0196971D-06    -2.4158147D-10     1.0107037D-14
     -2.2541024D-02     5.9822589D-05    -2.3113321D-08     3.1216035D-12    -1.4066207D-16
     -4.6511962D-03     2.2749974D-06    -4.0795574D-10     3.1712711D-14    -8.95773117D-19
      3.4397022D-05    -1.8883614D-08     3.8935996D-12    -3.5607856D-16     1.2158105D-20
*
*  *** Data for Bahadori Density Correlation
*
*     CO     Zero Density Coefficient [real]
*     C1     One Density Coefficient   [real]
*     C2     Two Density Coefficient   [real]
*     C3     Three Density Coefficient [real]
*
*     CO             C1             C2             C3

      208980.10      -1675.1824      4.4506010     -3.9198446D-03
      -14562.863      116.79955     -3.1043015D-01  2.7349738D-04
      288.58136      -2.3155834      6.1577189D-03 -5.4280074D-06
      -1.5971038      1.2840120D-02 -3.4203396D-05  3.0195721D-08
*
*     C4     Four Density Coefficient [real]
*     C5     Five Density Coefficient [real]
*     C6     Six Density Coefficient   [real]
*     C7     Seven Density Coefficient [real]
*
*     C4             C5             C6             C7

      105329.37      -825.33835      2.1357121     -1.8279565D-03
      -939.64485      7.6181258     -2.0231289D-02  1.7682977D-05
      2.3974143      -1.9635638D-02  5.2721255D-05 -4.6533771D-08
      -1.8190460D-03  1.4976584D-05 -4.0435641D-08  3.5867082D-11
```

APPENDIX 5

SUBROUTINE INJCDPDROP

```
C     *** START SUBROUTINE INJCDPDROP /NEW/
C
C     The program calculates Pressure drop in Reservoir due to Carbon
C     Dioxide Injection
C
       SUBROUTINE INJCDPDROP(PRS,TEMP,PORO,PERM,THICK,WIDTH,THETA,TBLK,
     +                       QINJCD,QCDBH,LOBS,LCDUD,LVFCD,LGCUD,
     +                       PDTOTCD,CATEGORYCD)
C
      IMPLICIT NONE
C
      CHARACTER*20 CATEGORYCD
C
      INTEGER NTAB
C
      REAL*8 PRS,TEMP,MWT,MWTG,MWTL,GASF,Z,Z2F,ZIN,ZCD,PRSINIT,PRSSC,
     +       TEMPRES,TEMPSC,PORO,PERM,THICK,WIDTH,THETA,TBLK,QINJCD,
     +       QCRITCD,QMAXCD,QCOND,QCDBH,ZBHCD,ZSCCD,MWCD,RGAS,PI,GRAV,
     +       LCDUD,LVFCD,LGCUD,LCDSD,MOBR,VISCCD,VISCGC,DENCD,DENGC,
     +       THCD,THGC,PDTOTCD,PDGCGS,PDCDGS,PDGCSD,PDCDSD,PDCDUD,
     +       PDGCUD,PDVFUD,XFUD,LOBS,LEEVISC,LIANGDEN,HEYVISC,BAHDEN,
     +       PRSTAB(50),TEMPTAB(50),MWTTAB(50),MWTGTAB(50),MWTLTAB(50),
     +       GASFTAB(50),ZTAB(50),Z2TAB(50),ZINTAB(50),ZCDTAB(50),
     +       BOTAB(50),B1TAB(50),B2TAB(50),B3TAB(50),B4TAB(50),
     +       B5TAB(50),B6TAB(50),B7TAB(50),B8TAB(50),B9TAB(50),
     +       COTAB(50),C1TAB(50),C2TAB(50),C3TAB(50),C4TAB(50),
     +       C5TAB(50),C6TAB(50),C7TAB(50)
C
      PARAMETER (RGAS=8.3142,MWCD=44.01,GRAV=9.806650,PI=3.141592654)
C
      COMMON /PVTDAT/ PRSTAB,TEMPTAB,GASFTAB,MWTTAB,MWTGTAB,MWTLTAB,
     +               ZTAB,Z2TAB,ZINTAB,ZCDTAB,NTAB
      COMMON /PTDAT/  PRSINIT,PRSSC,TEMPRES,TEMPSC
      COMMON /COEFDAT/ BOTAB,B1TAB,B2TAB,B3TAB,B4TAB,
     +                B5TAB,B6TAB,B7TAB,B8TAB,B9TAB
      COMMON /COEF2DAT/ COTAB,C1TAB,C2TAB,C3TAB,C4TAB,
     +                 C5TAB,C6TAB,C7TAB
C
C     CD= Carbon Dioxide        GC=Resident Gas: Gas Condensate
C
C     Density, Viscosity Calculation for Resident Gas and CO2
C
      CALL PVTTAB(PRS,TEMP,MWT,MWTG,MWTL,GASF,Z,Z2F,ZIN,ZCD)
      DENGC=100*PRS*MWT/(Z*RGAS*TEMP)           !kg/m^3
      DENCD=BAHDEN(PRS,TEMP,ZCD,MWCD)           !kg/m^3
      VISCGC=LEEVISC(MWT,PRS,TEMP,Z)            !bar-d
      VISCCD=HEYVISC(PRS,TEMP)                  !bar-d
      ZBHCD=ZCD
      CALL PVTTAB(PRS,TEMP,MWT,MWTG,MWTL,GASF,Z,Z2F,ZIN,ZCD)
      ZSCCD=ZCD
C
C     Injection Flow rate from SC to BH conditions for CO2 and Resident Gas
      QCDBH=PRSSC*QINJCD*ZBHCD*TEMP/(PRS*ZSCCD*TEMPSC)  ! Carbon Dioxide flow rate
      QCOND=(DENCD/DENGC)*QCDBH                         ! Gas condensate flow rate
C
C     Mobility Ratio Calculation
```

```
      MOBR=VISCGC/VISCCD
C
C     Maximum rate and critical rate for Carbon Dioxide Injection
      QMAXCD=86400*(PERM/VISCCD*1.0D+5*86400)*(DENCD-DENGC)*GRAV*WIDTH*
     +       THICK*(DSIN(ABS(THETA)*PI/180))/((1+SQRT(MOBR))**2)
      QCRITCD=86400*(PERM/VISCCD*1.0D+5*86400)*(DENCD-DENGC)*WIDTH*
     +       THICK*GRAV*(DSIN(ABS(THETA)*PI/180))/(1-MOBR)
C
C     Gravity Segregation Displacement
      THCD=THICK/(1+SQRT(MOBR))
      THGC=SQRT(MOBR)*THICK/(1+SQRT(MOBR))

      PDGCGS=-LOBS*(QCDBH*VISCGC/(PERM*WIDTH*THGC)+DENGC*GRAV*
     +       DSIN(ABS(THETA*PI/180))*1.0D-5)             !Pdrop in Gas Condensate Section (bar)
      PDCDGS=-LOBS*(QCDBH*VISCCD/(PERM*WIDTH*THCD)-
     +       DENCD*GRAV*DSIN(ABS(THETA)*PI/180)*1.0D-5)             !Pdrop in CO2 Section (bar)
C
C     Stable Displacement
      IF (MOBR.GE.1.01) THEN
      LCDSD=QCDBH*TBLK/(PORO*WIDTH*THICK*MOBR)                      !Carbon Dioxide length (m)
      ENDIF
      IF (MOBR.GE.0.AND.MOBR.LT.1.01) THEN
      LCDSD=QCDBH*TBLK*MOBR/(PORO*WIDTH*THICK)
      ENDIF
      PDGCSD=(QCOND*VISCGC/(PERM*WIDTH*THICK)-DENGC*GRAV*
     +    (DSIN(ABS(THETA)*PI/180))*1.0D-5)*(LOBS-LCDSD) !Pdrop in Gas Condensate Section (bar)
      PDCDSD=(QCDBH*VISCCD/(PERM*WIDTH*THICK)-DENCD*GRAV*
     +    (DSIN(ABS(THETA)*PI/180))*1.0D-5)*LCDSD                   !Pdrop in CO2 Section (bar)
C
C     Unstable Displacement
C
      IF (MOBR.GE.1.01) THEN
      LCDUD=QCDBH*TBLK/(PORO*WIDTH*THICK*MOBR)
      LVFCD=QCDBH*TBLK/(PORO*WIDTH*THICK)*(MOBR-1/MOBR)          ! Viscous Fingering Length (m)
      PDCDUD=QCDBH*VISCCD*LCDUD/(PERM*WIDTH*THICK)                ! Pdrop in CO2 section (bar)
      PDVFUD=-2/3*QCDBH**2*VISCGC*TBLK/((THICK*WIDTH)**2*PERM*PORO)*
     +       ((MOBR**2-1)**(3/2)/MOBR**2)            ! Pdrop in Viscous Fingering Section (bar)
      PDGCUD=QCOND*VISCGC*(LOBS-LCDUD-LVFCD)/(PERM*WIDTH*THICK)      ! Pdrop in Gas Condensate
C                                                                            Section (bar)
      ENDIF
C
      IF (MOBR.GE.0.AND.MOBR.LT.1.01) THEN
      LCDUD=QCDBH*TBLK*MOBR/(PORO*WIDTH*THICK)                     ! Carbon Dioxide Length (m)
C
      LGCUD=QCDBH*TBLK/(PORO*WIDTH*THICK*MOBR)                     ! Gas Condensate Length (m)
C
      PDCDUD=QCDBH*VISCCD*LCDUD/(PERM*WIDTH*THICK)                ! Pdrop in CO2 Section (bar)
C
      PDGCUD=QCOND*VISCGC*(LOBS-LCDUD)/(PERM*WIDTH*THICK)!Pdrop in Gas Condensate Section (bar)
C
      PDVFUD=0
      LVFCD=0
      ENDIF
C
C     Type of Displacement f (Reservoir inclination, flow rate)
      IF (THETA.GT.0) THEN
        IF(QCDBH.GT.QMAXCD) GOTO 131
        IF(QCDBH.LE.0) GOTO 144
        GOTO 133
      ELSE IF (THETA.LT.0) THEN
        IF (QCDBH.GT.QCRITCD) GOTO 131
        IF (QCDBH.LE.0) GOTO 144
```

```
        GOTO 132
      ELSE IF (THETA.EQ.0) THEN
        IF (QCDBH.LE.0) GOTO 144
        GOTO 131
      ENDIF
C
  131 CONTINUE
      CATEGORYCD='UNSTABLE'                    ! Unstable Displacement
      IF (LOBS.GT.(LGCUD+LVFCD+LCDUD)) THEN
        PDTOTCD=PDCDUD+PDVFUD+PDGCUD
      ELSE IF ((LOBS.GT.LCDUD).AND.(LOBS.LE.(LGCUD+LVFCD+LCDUD))) THEN
        IF (MOBR.GT.1.01) THEN
        PDTOTCD=PDCDUD+PDVFUD*((LOBS-LCDUD)/LVFCD)
        ENDIF
        IF (MOBR.LT.1.01) THEN
        PDTOTCD=PDCDUD
        ENDIF
      ELSE IF (LOBS.LE.LCDUD) THEN
        PDTOTCD=PDCDUD*(LOBS/LCDUD)
      ENDIF
      RETURN
C
  132 CONTINUE
      CATEGORYCD='STABLE'                      ! Stable Displacement
      IF (LOBS.LT.LCDSD) THEN
        PDTOTCD=PDCDSD*(LOBS/LCDSD)
      ELSE
        PDTOTCD=PDGCSD+PDCDSD
      ENDIF
      RETURN
C
  133 CONTINUE
      CATEGORYCD='GRAVITY SEG'                 ! Gravity Segregation Displacement
      PDTOTCD=PDGCGS+PDCDGS
      RETURN
C
  144 CONTINUE
      PDTOTCD=0                                ! No CO2 Injection
      IF (PDTOTCD.EQ.0) CATEGORYCD=' '
      RETURN
C
      END
C
C     *** END SUBROTUINE INJCDPDROP /NEW/
C
C ****************************************************************
```